Electronic Supplementary Information

Synthesis of all-aliphatic polyamide dendrimers based on a 3,3´-diaminopivalic acid scaffold

Antonio J. Ruiz-Sanchez,[ab‡] Pablo Mesa-Antunez,[ab‡] Nekane Barbero,[ab] Daniel Collado,[ab] Yolanda Vida,[ab] Francisco Najera,[ab] Ezequiel Perez-Inestrosa[,ab]*

[a]*Universidad de Malaga, IBIMA, Department of Organic Chemistry, 29071-Malaga, Spain.*
[b]*Andalusian Centre for Nanomedicine and Biotechnology-BIONAND, Parque Tecnologico de Andalucia, 29590-Malaga, Spain.*
[‡]*These authors contributed equally.*

Table of Contents.

1. General Methods

1.1. Materials

All reagents and solvents were used as received without further purification. Where dry solvents were needed, water was removed according to the literature procedure.[1]

3,3'-Dichloropivalic acid, thionyl chloride ($SOCl_2$), ethylendiamine, 10% Pd/C and 4-(dimethylamino)pyridine (DMAP) were obtained from Sigma-Aldrich. Dimethylformamide (DMF), sodium azide (NaN_3), dichloromethane (CH_2Cl_2), methanol (MeOH), ethyl acetate (EtOAc), *n*-hexane 95%, formic acid, hydrochloric acid (HCl), magnesium sulfate ($MgSO_4$), Celite® and sodium hydroxide (NaOH) were obtained from Merck.

1.2. Instrumentation

Thin layer chromatography (TLC) was performed using silica gel plates (SDS, 60 F_{254}). They were developed using UV light (254 nm) or chemical developing agents such as potassium permanganate, bromocresol green, phosphomolybdic acid or ninhydrin. Column chromatography purification was carried out using silica gel (Merck, silica gel 60, 0.040-0.063 mm, 230-400 mesh) for flash chromatography and silica gel (Merck, silica gel 60, 0.063-0.200 mm, 70-2230 mesh) for gravity columns. The solvent employed is shown in each case. Nuclear Magnetic Resonance (NMR) spectra were obtained using a Bruker WP-200 SY at 200 MHz for ^{1}H and 50.3 MHz for ^{13}C, a Bruker ARX-400 at 400 MHz for ^{1}H and 100.6 MHz for ^{13}C or a Bruker Biospin Avance III 400 at 400 MHz for ^{1}H and 100.6 MHz for ^{13}C. The chemical shifts (δ, ppm) are relative to the residual deuterated solvent signal in each case.[2] Mass spectra were performed in a Thermo Scientific DSQ II Single Quadrupole GC/MS with Focus GC mass spectrometer with electronic impact ionization (70 eV). HRMS (FAB and ESI-TOF) were obtained using a VG Autospec spectrometer. MALDI-TOF measurements were acquired using a 4700 Proteomics Analyzer mass spectrometer (ABSCIEX, Foster City, CA, USA) working in reflector positive or linear positive ion mode. Elemental analyses were performed using a LECO CHNS-932 Elemental Analyzer. Infrared (IR) spectra were recorded using a Bruker FTIR Vertex70 spectrophotometer with a Golden Gate Single Reflection Diamond ATR System (ν_{max} in cm^{-1}). Hydrogenation reactions were carried out under hydrogen atmosphere (20 bar) using a 100 mL Mini-Reactor from Parker-Autoclave Engineers.

2. Synthesis of BAPAD Dendrimers

2.1. Synthesis of 3,3'-diazidopivalic acid (1)

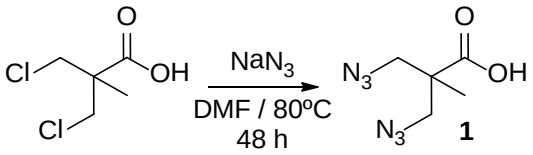

A mixture of 3,3'-dichloropivalic acid (4.0 g, 23.4 mmol) and NaN_3 (6.1 g, 93.8 mmol) in DMF:H_2O (9:1, 10 mL) was stirred at 80 ºC for 48 h. The mixture was then cooled to room temperature, filtered and the solvent removed under vacuum. The residue was purified by silica gel column chromatography (ethyl acetate/hexane/formic acid: 1/4/0.01) giving the desired compound as a colorless oil (78% yield). δ_H (400 MHz; $CDCl_3$) 11.86 (1H, s, COO*H*), 3.61 (2H, d, *J* = 12.2 Hz, N_3CHH), 3.50 (2H, d, *J* = 12.2 Hz, N_3CHH), 1.25 (3H, s, CCH_3). δ_C (100 MHz; $CDCl_3$) 179.9, 54.4, 47.4, 19.1. Anal. Calcd. C, 32.61; H, 4.38; N, 45.64, found: C, 32.63, H, 4.40; N 45.61 for $C_5H_8N_6O_2$.

2.2. Synthesis of 3,3'-diazidopivaloyl chloride (2)

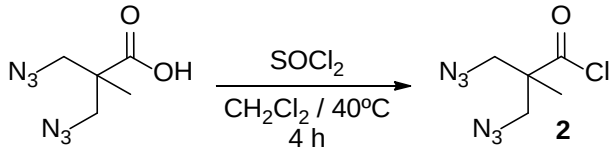

Thionyl chloride (4.0 mL) was added dropwise at room temperature to a solution of 3,3'-diazidopivalic acid (3.3 g, 17.9 mmol) in CH_2Cl_2 (20 mL). The reaction was heated to 40ºC for 4 hours and then concentrated to afford quantitatively 3,3'-diazidopivaloyl chloride as a yellow oil, which was used directly without further purification. δ_H (400 MHz; $CDCl_3$) 3.68 (2H, d, *J* = 12.5 Hz, N_3CHH), 3.60 (2H, d, *J* = 12.5 Hz, N_3CHH), 1.34 (3H, s, CCH_3). δ_C (100 MHz; $CDCl_3$) 175.6, 57.0, 54.4, 19.0.

2.3. G1-N_3 Synthesis

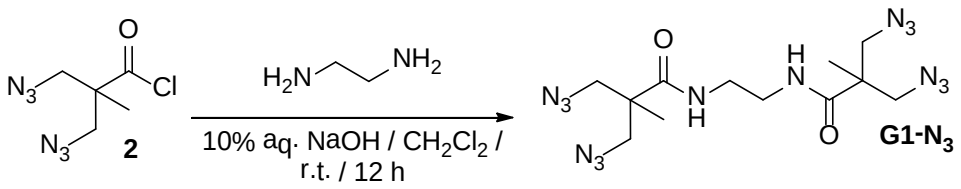

A mixture of ethylendiamine (0.408 g, 6.8 mmol), 20 mL of CH_2Cl_2 and 20 mL of 10% aqueous sodium hydroxide was cooled to 0 ºC. To this, freshly prepared **2** (3.04 g, 15 mmol) in CH_2Cl_2 (50 mL) was added dropwise using a pressure-equalizing dropping funnel while its temperature was kept to 0 ºC. After addition, the reaction was allowed to reach room temperature and stirred overnight. The organic layer was then separated, washed with 10% aqueous sodium hydroxide, 1 M aqueous HCl and water, dried over anhydrous $MgSO_4$ and the solvent removed. Purification by silica gel column chromatography (EtOAc/Hexane: 1/1) gave the desired compound as a white solid (78% yield). δ_H (400 MHz; $CDCl_3$) 6.82 (2H, bs, N*H*), 3.56 (4H, d, *J* = 12.2 Hz, H_c), 3.47 (4H, d, *J* = 12.2 Hz, H_c), 3.44 (4H, m, H_a), 1.26 (6H, s, H_b). δ_C (100 MHz; $CDCl_3$) 174.0, 55.9, 47.2, 40.4, 18.8. IR (neat, cm^{-1}): 3334 (br), 2959 (m), 2933 (m), 2872 (m), 2095 (vs), 1737 (w), 1635 (s), 1536 (s). ESI-TOF HRMS (*m/z*): Calcd. 393.19664, found: 393.19645 for $C_{12}H_{21}N_{14}O_2$ $[M+H]^+$.

2.4. Synthesis of G1-NH_2

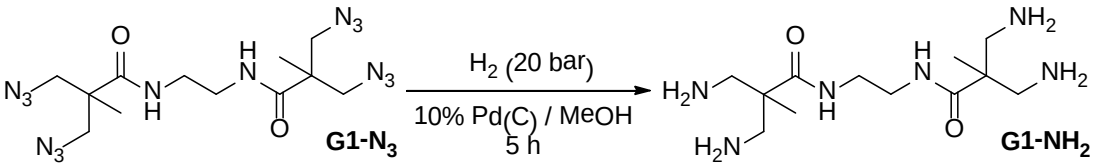

G1-N_3 (0.550 g, 1.4 mmol) was dissolved in MeOH (30 mL) and the solution shaken under a hydrogen atmosphere (20 bar) in the presence of 10% Pd/C (20 mg) for 5 hours. The catalyst was filtered off through Celite® and washed with methanol. The filtrate was concentrated under vacuum to yield the desired compound as a colorless oil (quantitative yield). δ_H (400 MHz; $(CD_3)_2SO$) 8.51 (2H, bs, N*H*), 3.14 (4H, s, H_a), 2.70 (8H, s, NH_2), 2.64 (4H, d, *J* = 12.8 Hz, H_c), 2.58 (4H, d, *J* = 12.8 Hz, H_c), 0.95 (6H, s, H_b). δ_C (100 MHz; $(CD_3)_2SO$) 176.5, 47.3, 47.2, 38.6, 19.3. IR (neat, cm^{-1}): 3286 (br), 2965 (m), 2923 (m), 2854 (m), 1734 (w), 1629 (s), 1529 (s). ESI-TOF HRMS (*m/z*): Calcd. 289.23465, found: 289.23527 for $C_{12}H_{29}N_6O_2$ $[M+H]^+$.

2.5. Synthesis of G2-N_3

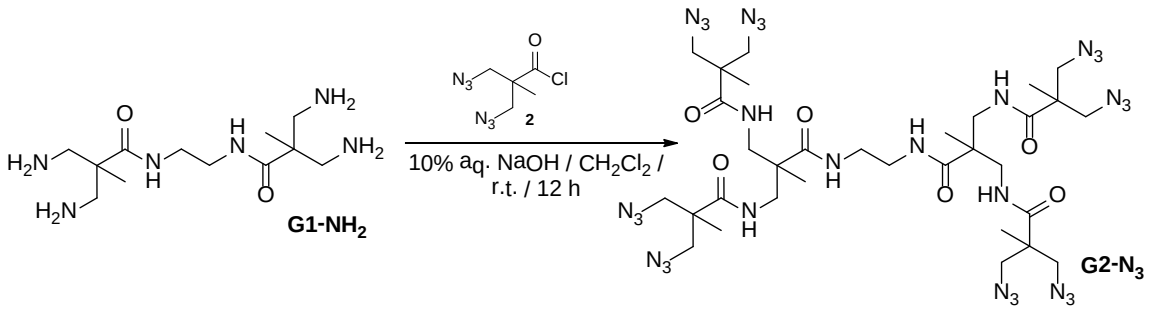

A mixture of **G1-NH_2** (0.400 g, 1.4 mmol), 10 mL of CH_2Cl_2 and 10 mL of 10% aqueous sodium hydroxide was cooled to 0 ºC. To this, freshly prepared **2** (2.262 g, 11.2 mmol) in CH_2Cl_2 (20 mL) was added dropwise with a pressure-equalizing dropping funnel while its temperature was kept to 0 ºC. After addition, the temperature was allowed to reach room temperature and stirred overnight. The organic layer was then separated, washed with 10% aqueous sodium hydroxide, 1 M aqueous HCl and water, dried over anhydrous $MgSO_4$ and the solvent removed. Purification by crystallization (EtOAc/Hexane: 3/1) gave the desired compound as a white solid (39% yield). δ_H (400 MHz; $CDCl_3$) 7.56 (2H, bs, N*H*), 7.36 (4H, t, *J* = 6.6 Hz, N*H*), 3.65 (4H, dd, *J* = 14.2, 6.6 Hz, H_c), 3.60-3.49 (16H, m, H_e), 3.29 (4H, bs, H_a), 3.24 (4H, dd, *J* = 14.2, 6.6 Hz, H_c), 1.29 (12H, s, H_d), 1.19 (6H, s, H_b). δ_C (100 MHz; $CDCl_3$) 174.9, 174.1, 56.2, 56.0, 47.5, 47.4, 42.7, 39.6, 20.0, 19.2. IR (neat, cm^{-1}): 3293 (br), 2972 (m), 2936 (m), 2876 (m), 2094 (vs), 1735 (w), 1634 (s), 1542 (s). ESI-TOF HRMS (*m/z*): Calcd. 953.47589, found: 953.47893 for $C_{32}H_{53}N_{30}O_6$ $[M+H]^+$.

2.6. Synthesis of G2-NH_2

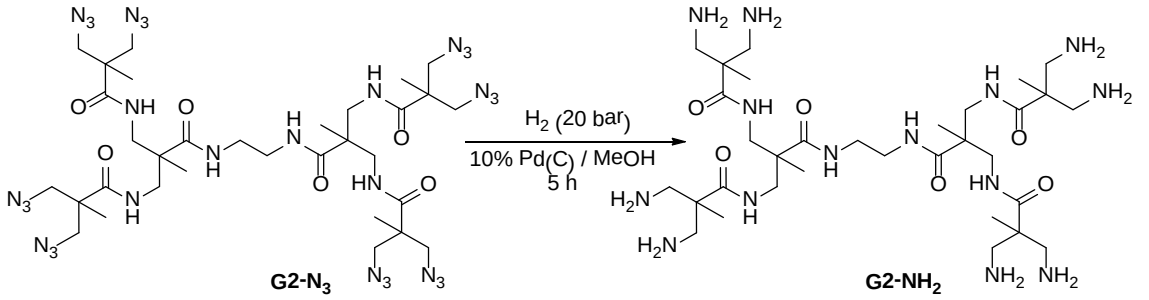

G2-N_3 (0.230 g, 0.24 mmol) was dissolved in MeOH (10 mL) and the solution shaken under a hydrogen atmosphere (20 bar) in the presence of 10% Pd/C (15 mg) for 5 hours. The catalyst was filtered off through Celite® and washed with methanol. The filtrate

was concentrated in vacuum to yield the desired compound as a colorless oil (quantitative yield). δ_H (400 MHz; $(CD_3)_2SO$) 8.85 (4H, bs, N*H*), 7.95 (2H, bs, N*H*), 3.65-3.50 (4H, m. H_c), 3.13-2.95 (8H, m, H_a, H_c), 2.66 (8H, d, J = 12.8 Hz, H_e), 2.60 (8H, d, J = 12.8 Hz, H_e), 1.07 (6H, s, H_b), 0.96 (12H, s, H_d). δ_C (100 MHz; $(CD_3)_2SO$) 176.9, 174.3, 47.5, 47.3, 47.0, 42.5, 38.4, 19.3, 19.2. IR (neat, cm^{-1}): 3285 (br), 2968 (m), 2935 (m), 2875 (m), 1720 (w), 1632 (s), 1534 (s). ESI-TOF HRMS (*m/z*): Calcd. 745.55190, found: 745.55118 for $C_{32}H_{69}N_{14}O_6$ $[M+H]^+$.

2.7. Synthesis of G3-N_3

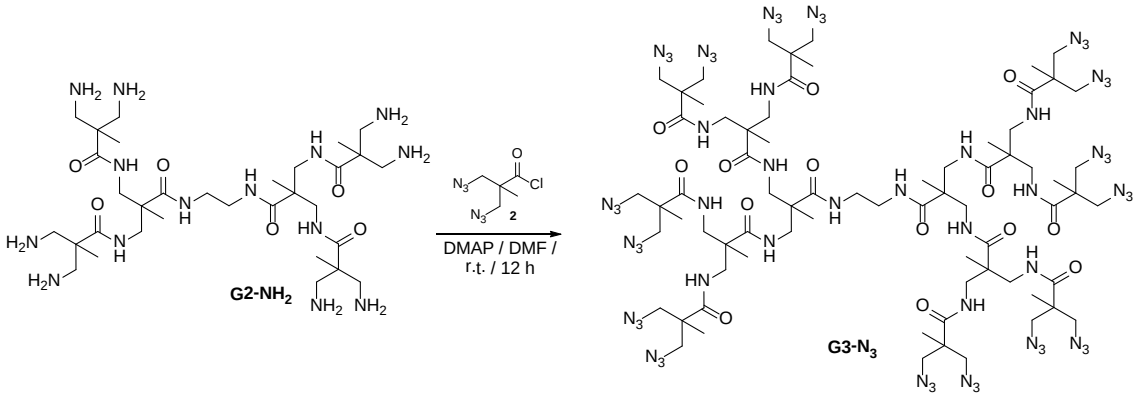

Freshly prepared **2** (0.780 g, 3.8 mmol) in dry DMF (10 mL) was slowly added dropwise to a mixture of **G2-NH_2** (0.18 g, 0.24 mmol) and DMAP (0.470 g, 3.8 mmol) in 10 mL of dry DMF under an argon atmosphere and stirred at room temperature overnight. The solvent was removed under vacuum and the residue dissolved in CH_2Cl_2. The organic layer was washed with 1 M aqueous HCl, 10% aqueous sodium hydroxide and water, dried over anhydrous $MgSO_4$ and the solvent removed. Purification by silica gel column chromatography (EtOAc/Hexane 4/1) gave the desired compound as a colorless oil (27% yield). δ_H (400 MHz; $CDCl_3$) 8.19-7.44 (14H, m, N*H*), 3.79-3.49 (44H, m, H_c, H_e, H_g), 3.32-3.19 (16H, m, H_a, H_c, H_e), 1.35-1.12 (42H, m, H_b, H_d, H_f). δ_C (100 MHz; $CDCl_3$) 176.0, 174.9, 174.2, 56.0, 47.9, 47.6, 46.9, 46.5, 43.1, 42.4, 37.6, 20.0, 19.1, 18.6. ESI-TOF HRMS (*m/z*): Calcd. 1037.52082, found: 1037.51988 for $C_{72}H_{118}N_{62}O_{14}$ $[M+2H]^{2+}$.

2.8. Synthesis of G3-NH_2

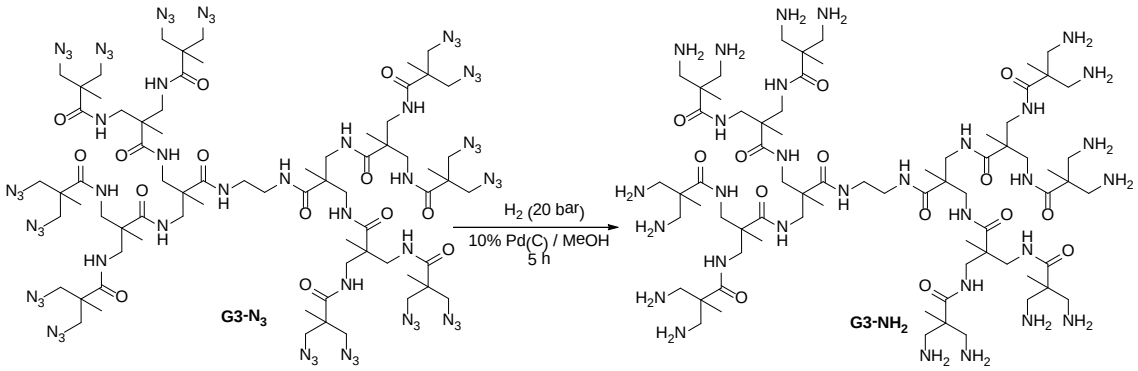

G3-N_3 (0.080 g, 0.04 mmol) was dissolved in MeOH (10 mL) and the solution shaken under a hydrogen atmosphere (20 bar) in the presence of 10% Pd/C (15 mg) for 5 hours. The catalyst was filtered off through Celite® and washed with methanol. The filtrate was concentrated in vacuum to yield the desired compound as a colorless oil (quantitative yield). δ_H (400 MHz, $(CD_3)_2SO$) 8.90-7.40 (14H, m, N*H*), 3.96-2.85 (28H, m, H_a, H_c, H_e), 2.72-2.54 (32H, m, H_g), 1.23-0.73 (42H, m, H_b, H_d, H_f). δ_C (100 MHz; $(CD_3)_2SO$) 176.7, 176.0, 175.3, 47.6, 47.3, 42.6 42.5, 19.3, 19.1. MALDI-TOF MS (*m/z*): Calcd. 1658.186, found: 1658.149 for $C_{72}H_{149}N_{30}O_{14}$ $[M+H]^+$; 1680.192 for $C_{72}H_{148}N_{30}O_{14}Na$ $[M+Na]^+$; 1696.19714 for $C_{72}H_{148}N_{30}O_{14}K$ $[M+K]^+$.

3. NMR and Mass spectra

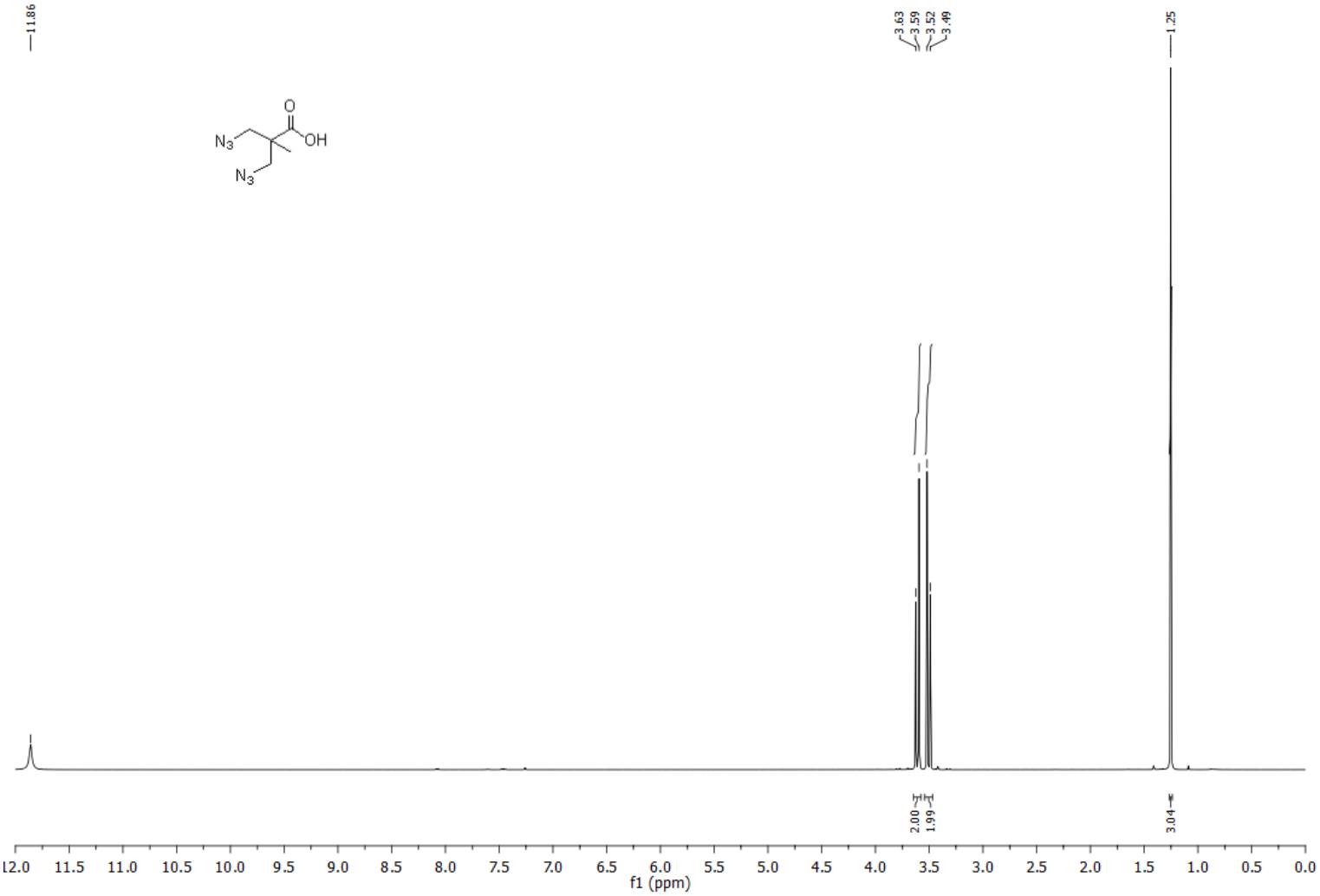

Fig. S1 ^{1}H-NMR spectrum (400 MHz, $CDCl_3$) of compound **1**.

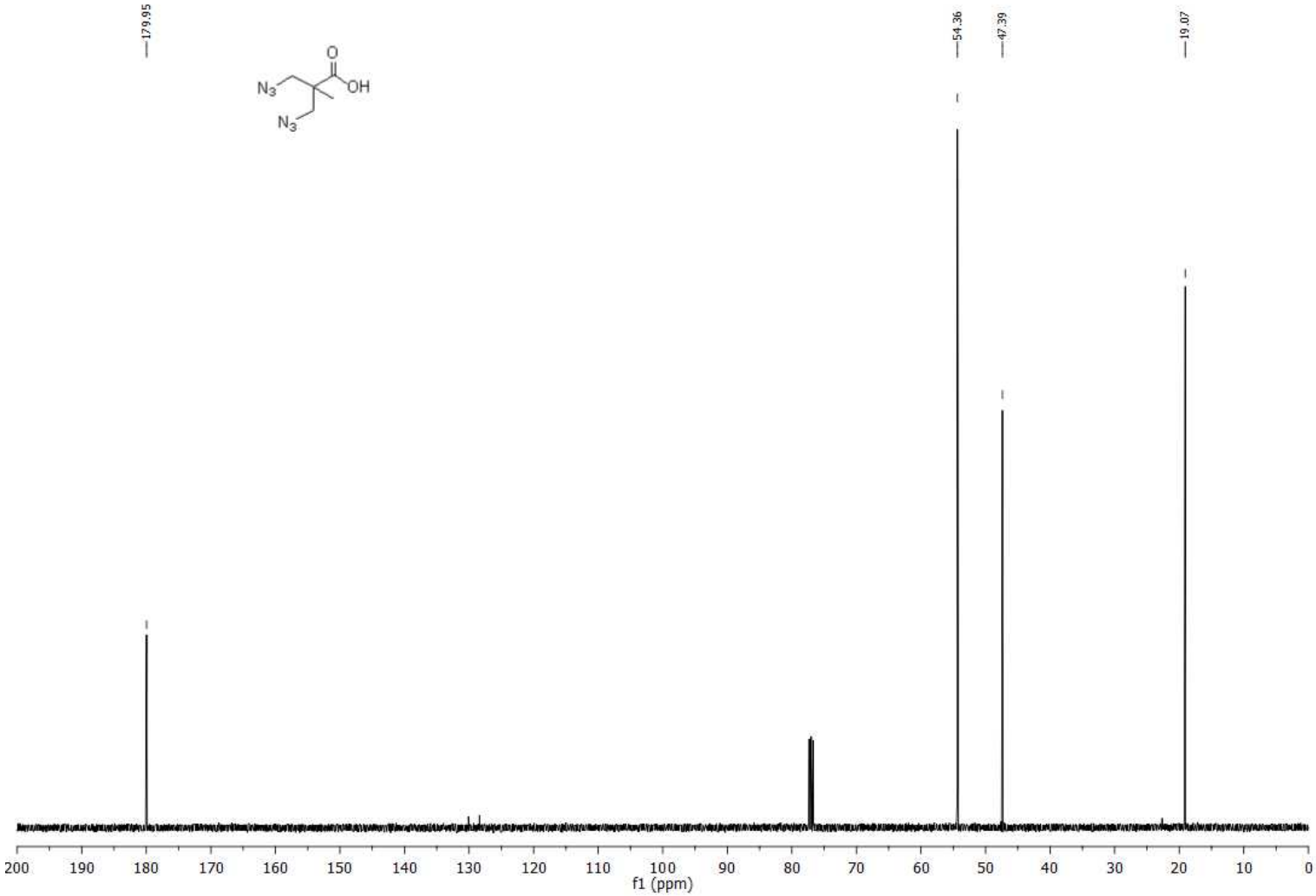

Fig. S2 ^{13}C-NMR spectrum (100 MHz, $CDCl_3$) of compound **1**.

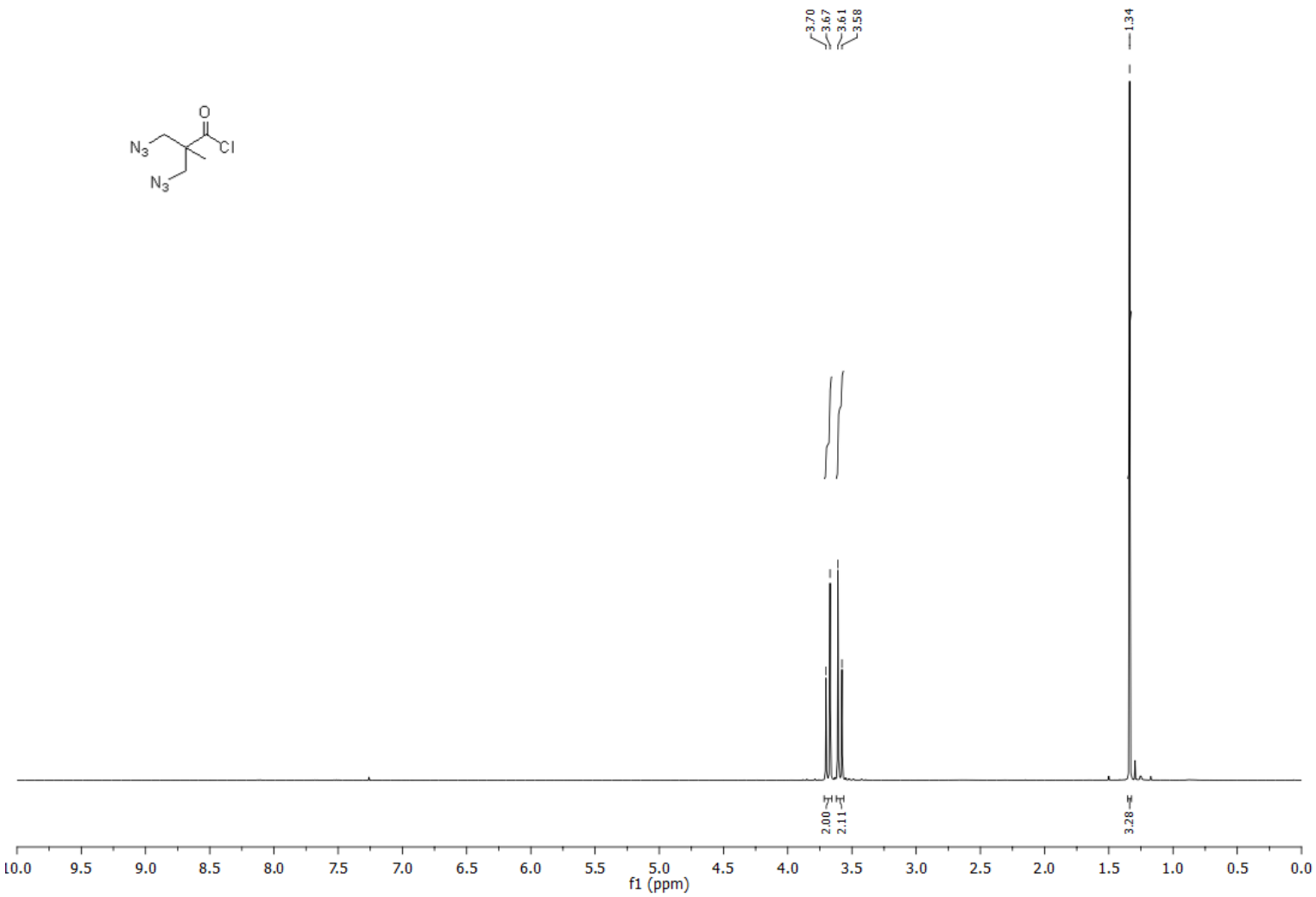

Fig.S3 ^{1}H-NMR spectrum (400 MHz, $CDCl_3$) of compound **2**.

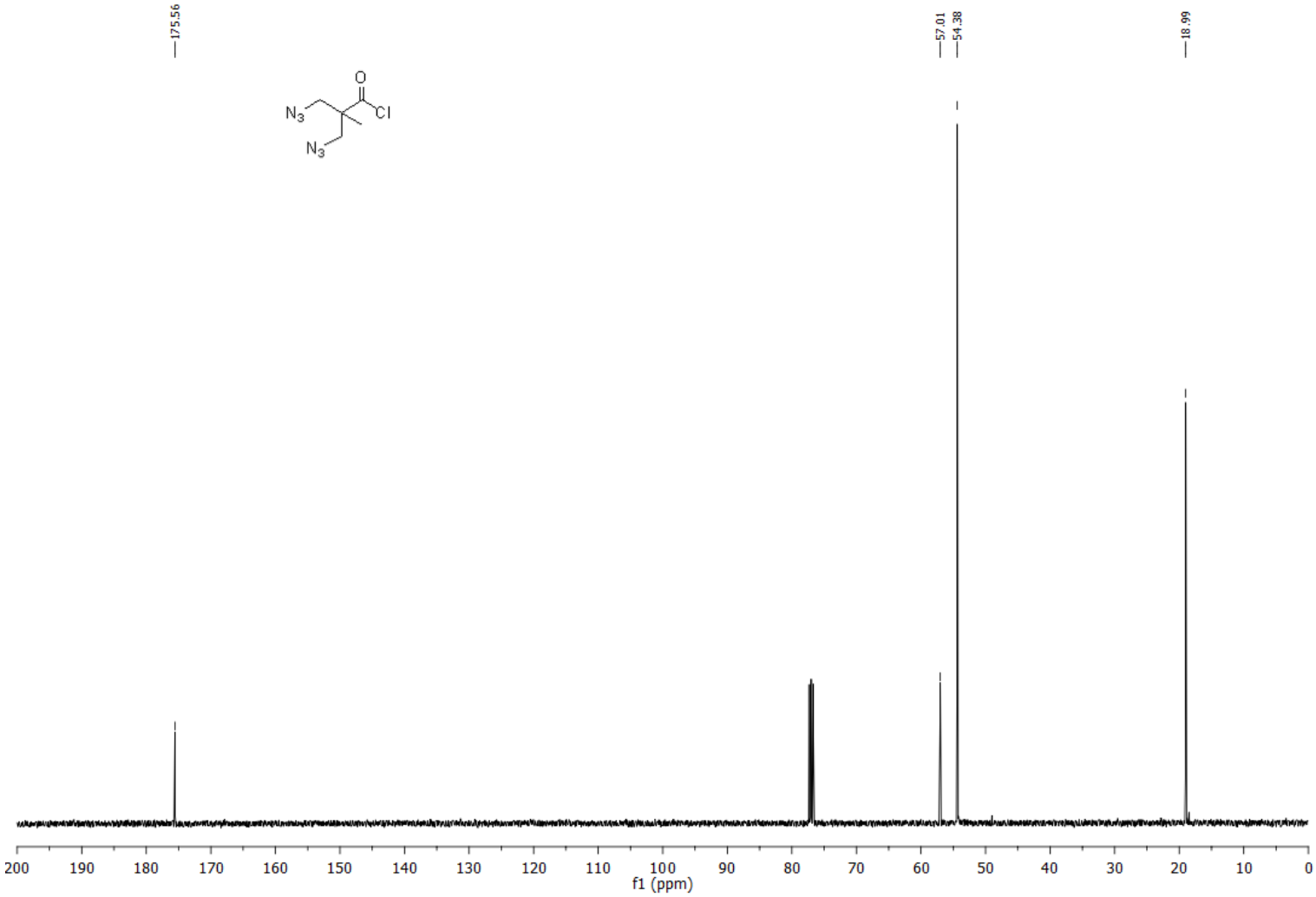

Fig. S4 ^{13}C-NMR spectrum (100 MHz, $CDCl_3$) of compound **2**.

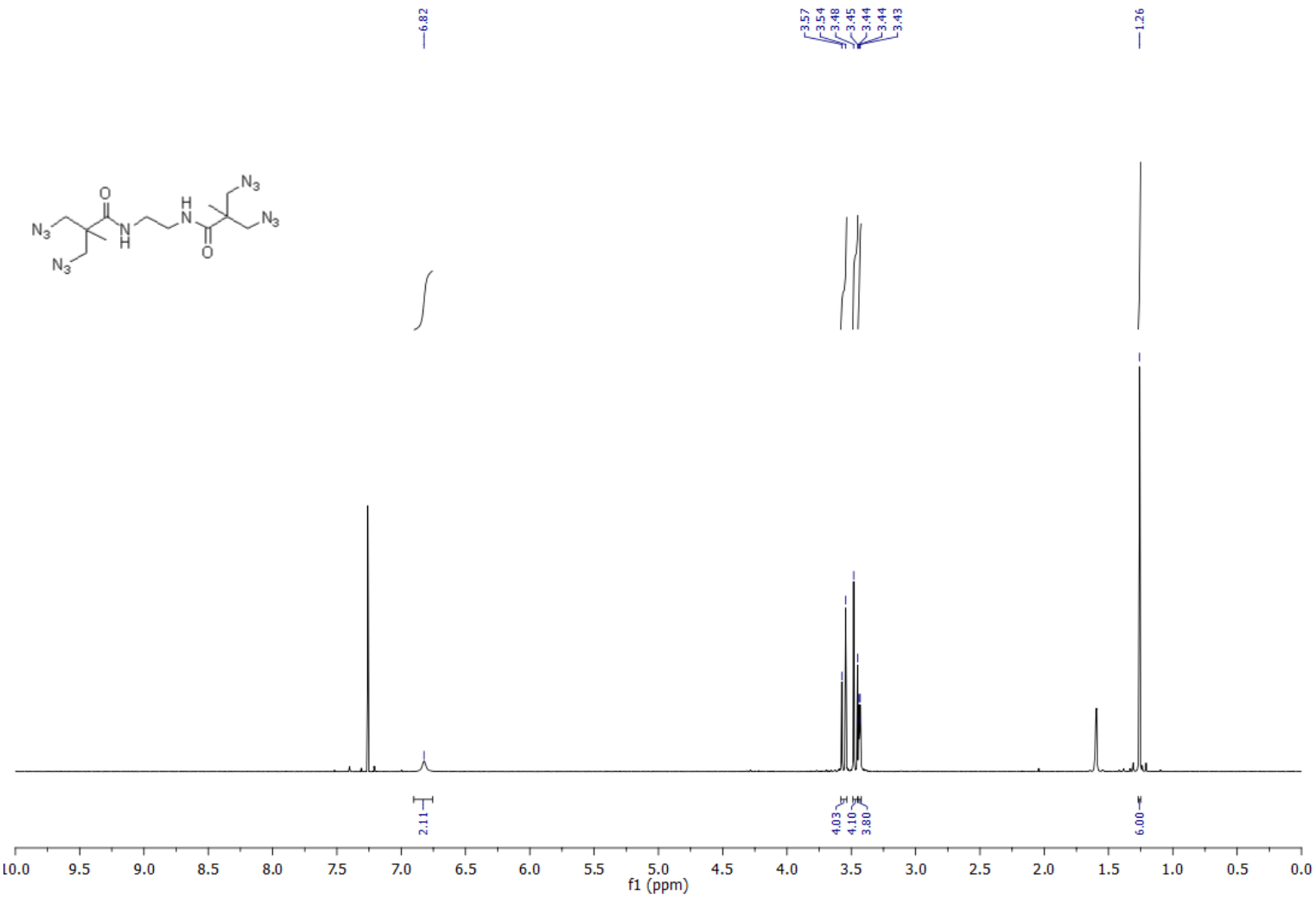

Fig. S5 ^{1}H-NMR spectrum (400 MHz, $CDCl_3$) of **G1-N_3**.

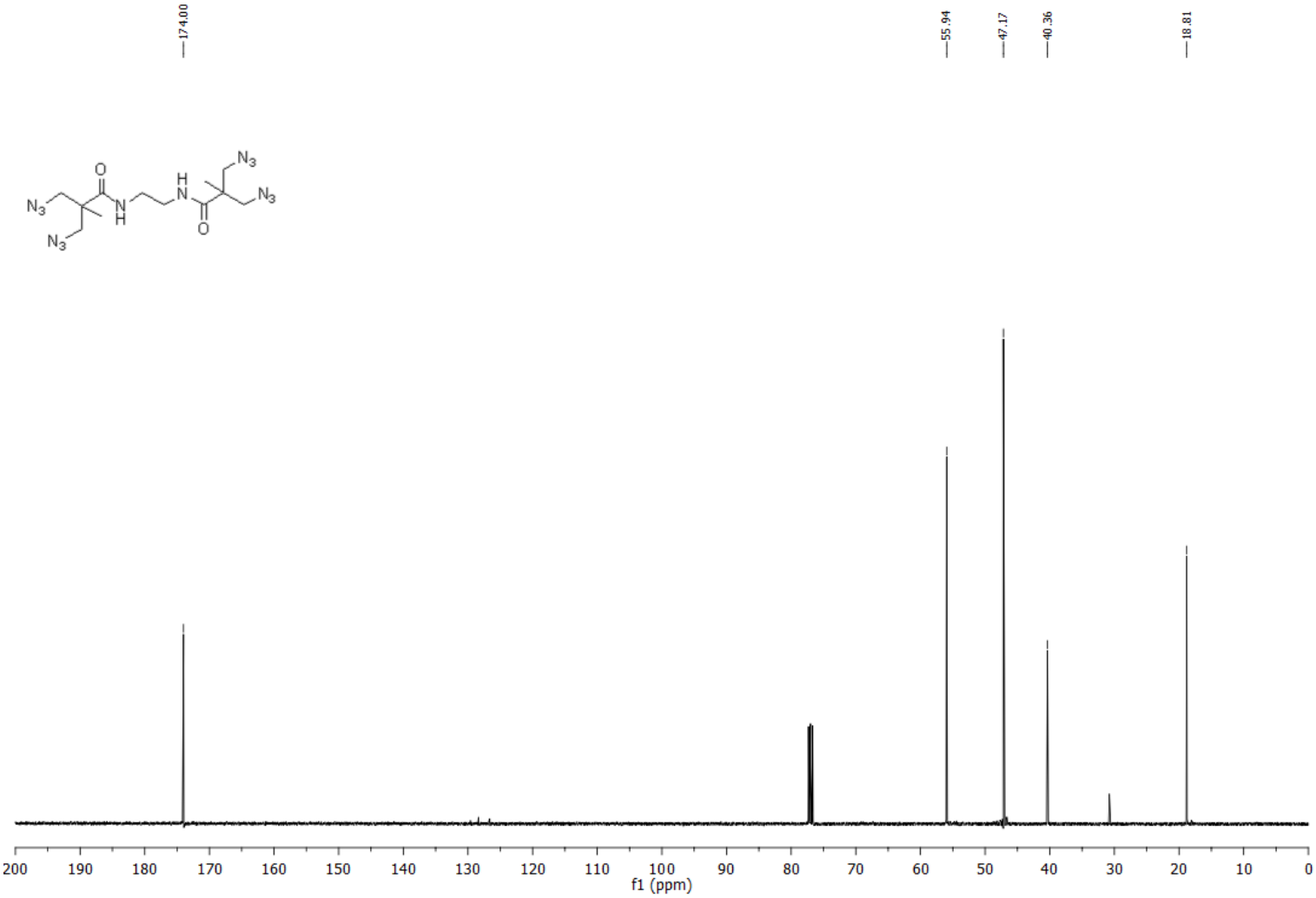

Fig. S6 ^{13}C-NMR spectrum (100 MHz, $CDCl_3$) of **G1-N_3**.

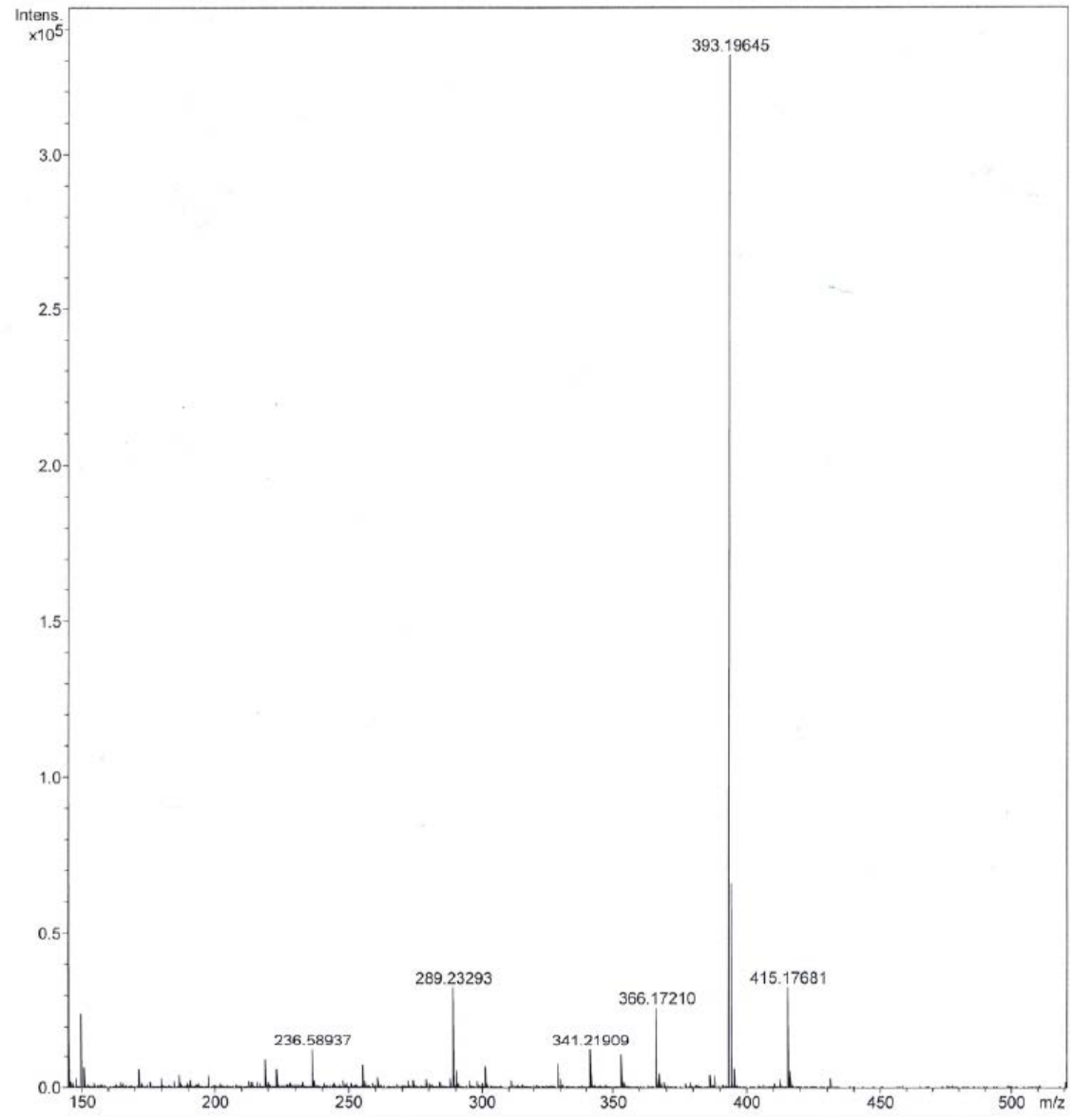

Mass Spectrum Molecular Formula Report

Meas. m/z	#	Formula	Score	m/z	err [mDa]	err [ppm]	mSigma	rdb	e⁻ Conf	N-Rule
393.19345	1	C 12 H 21 N 14 O 2	100.00	393.19664	0.2	0.5	10.6	9.5	even	ok
415.17381	1	C 12 H 20 N 14 Na O 2	100.00	415.17859	1.8	4.3	11.8	9.5	even	ok

Fig. S7 ESI-TOF spectrum and Mass spectrum molecular formula report of **G1-N_3**.

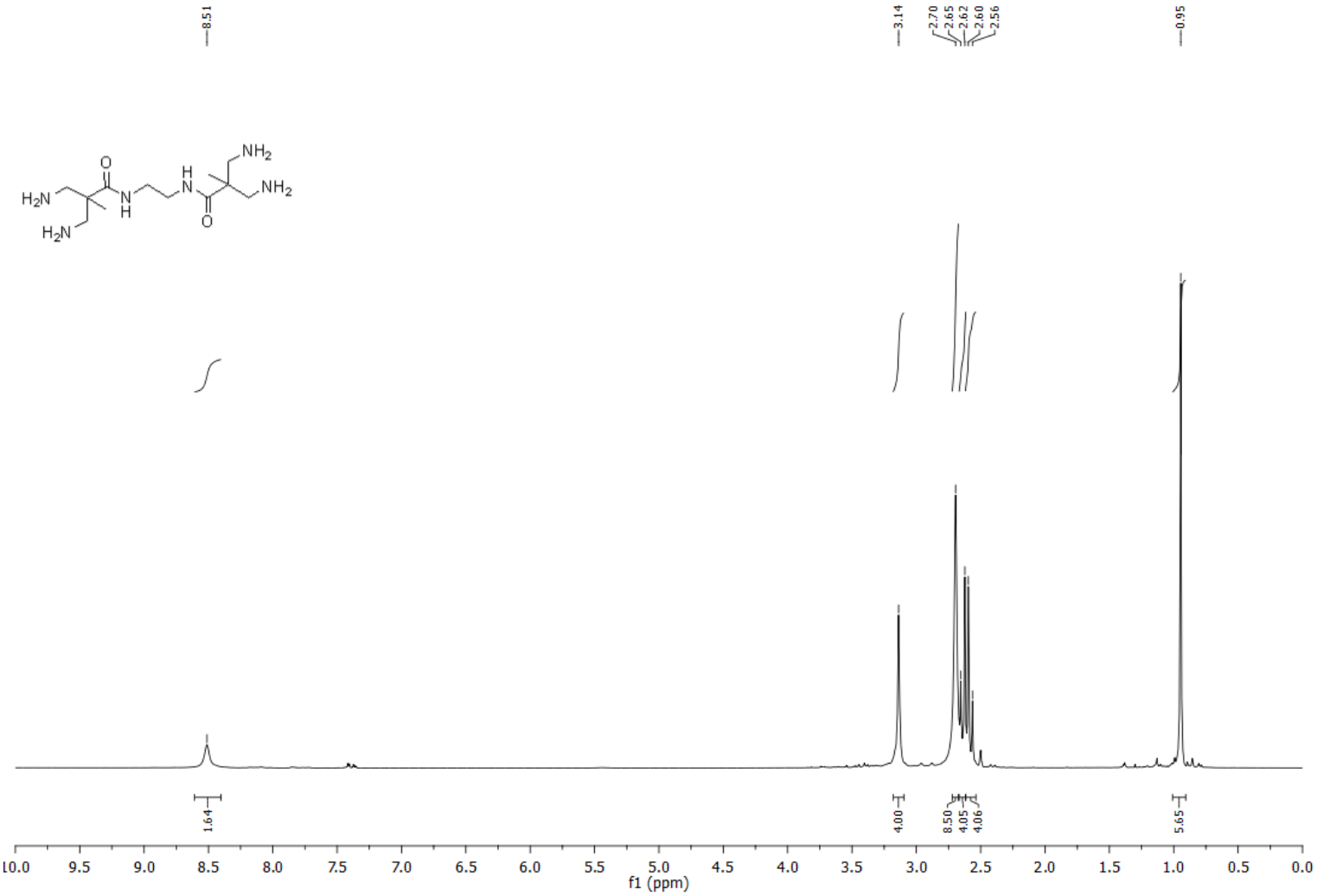

Fig. S8 ^{1}H-NMR spectrum (400 MHz, $(CD_3)_2SO$) of **G1-NH$_2$**.

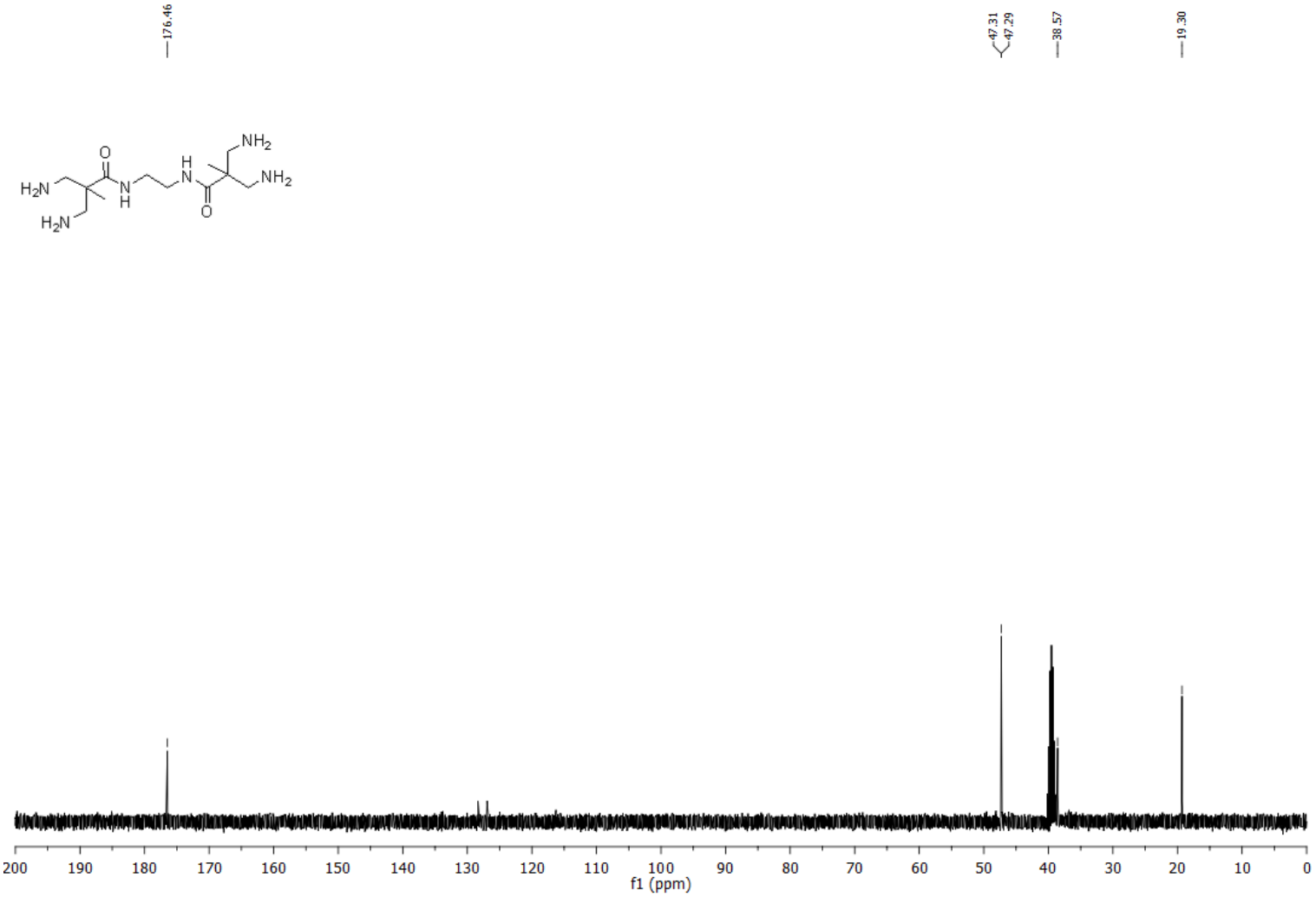

Fig. S9 ^{13}C-NMR spectrum (100 MHz, $(CD_3)_2SO$) of **G1-NH$_2$**.

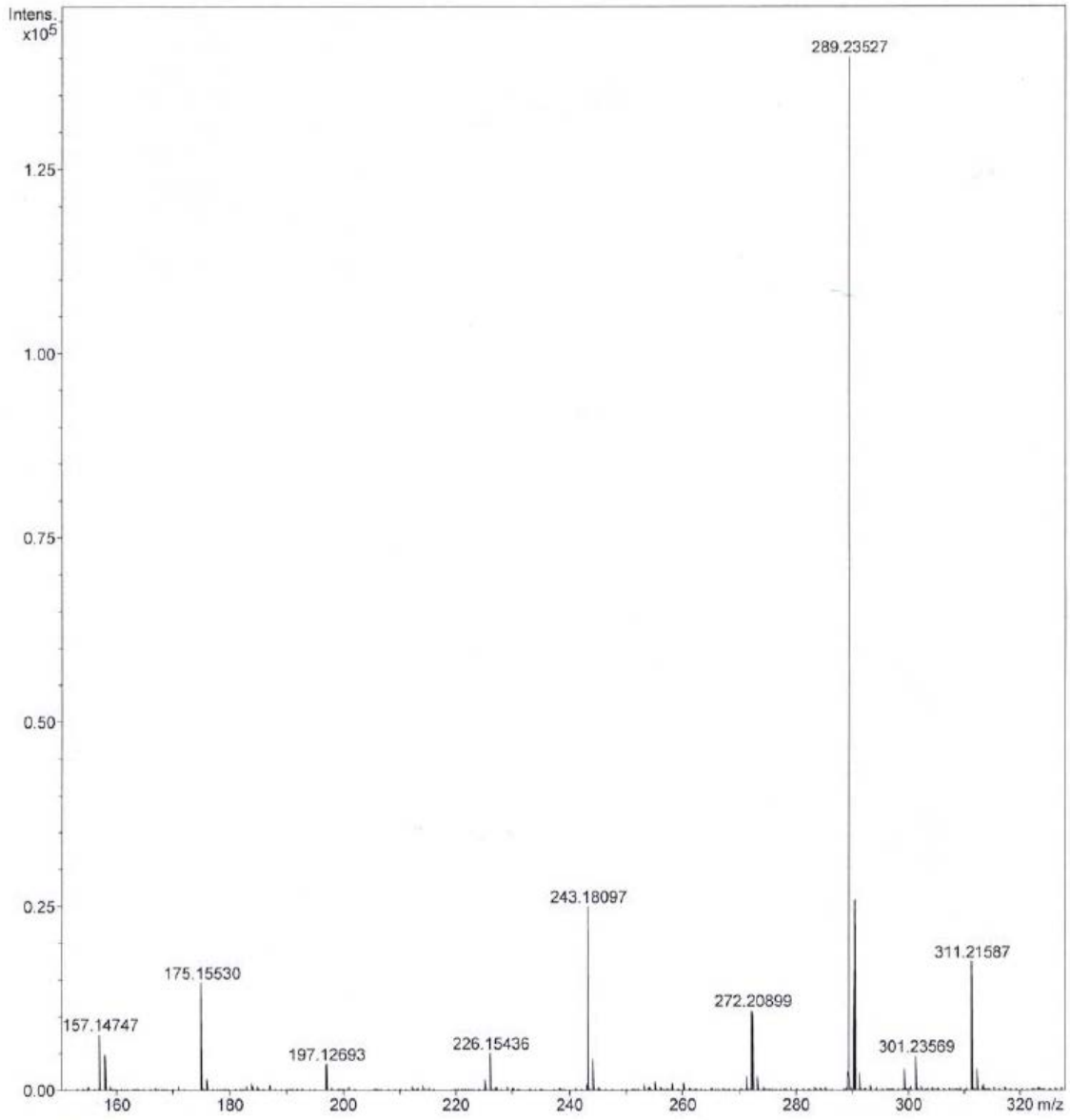

Mass Spectrum Molecular Formula Report

Meas. m/z	#	Formula	Score	m/z	err [mDa]	err [ppm]	mSigma	rdb	e⁻ Conf	N-Rule
289.23527	1	C 12 H 29 N 6 O 2	100.00	289.23465	-0.6	-2.1	18.7	1.5	even	ok
311.21587	1	C 12 H 28 N 6 Na O 2	100.00	311.21660	0.7	2.3	11.2	1.5	even	ok

Fig. S10 ESI-TOF spectrum and Mass spectrum molecular formula report of **G1-NH_2**.

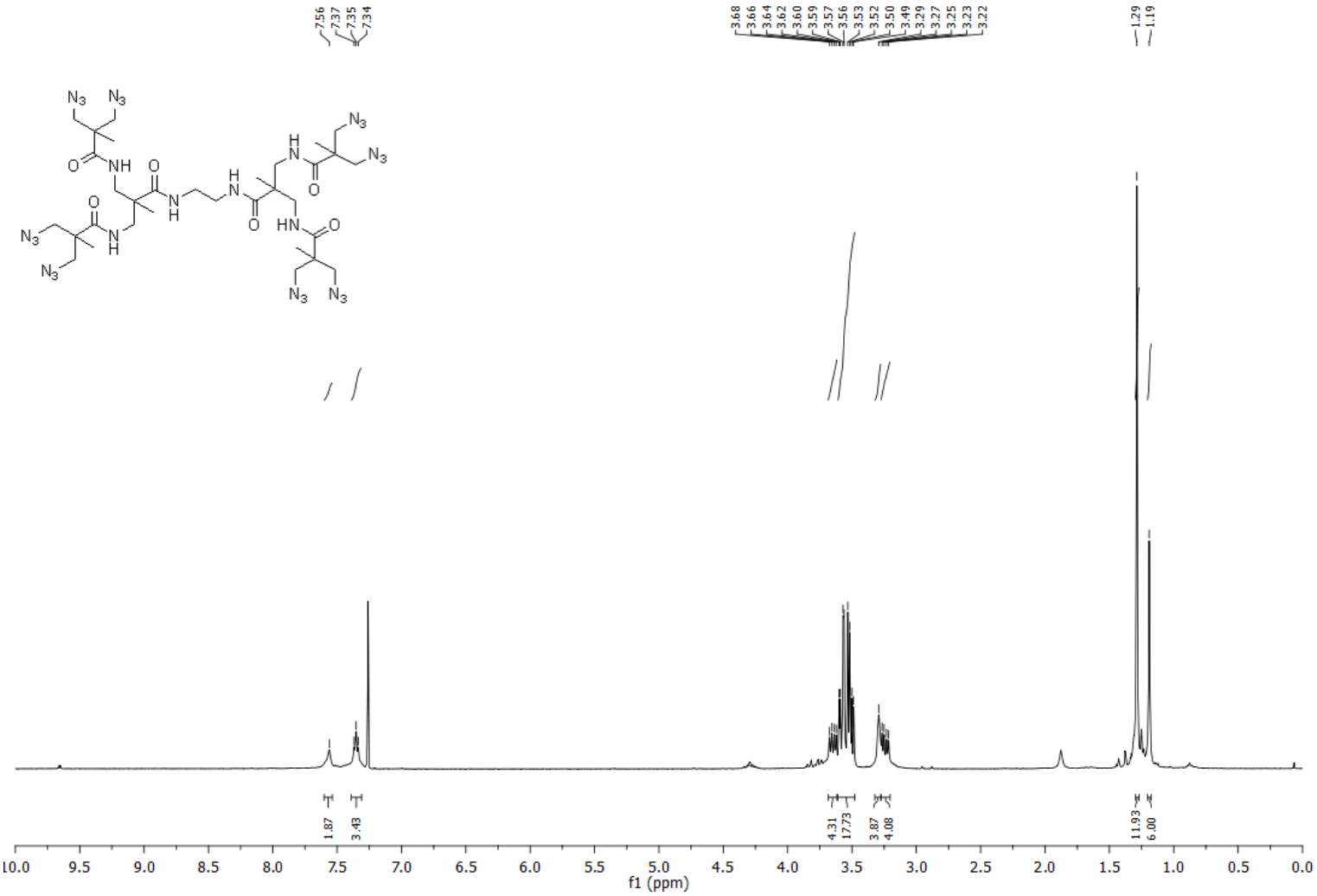

Fig. S11 ^{1}H-NMR spectrum (400 MHz, $CDCl_3$) of **G2-N_3**.

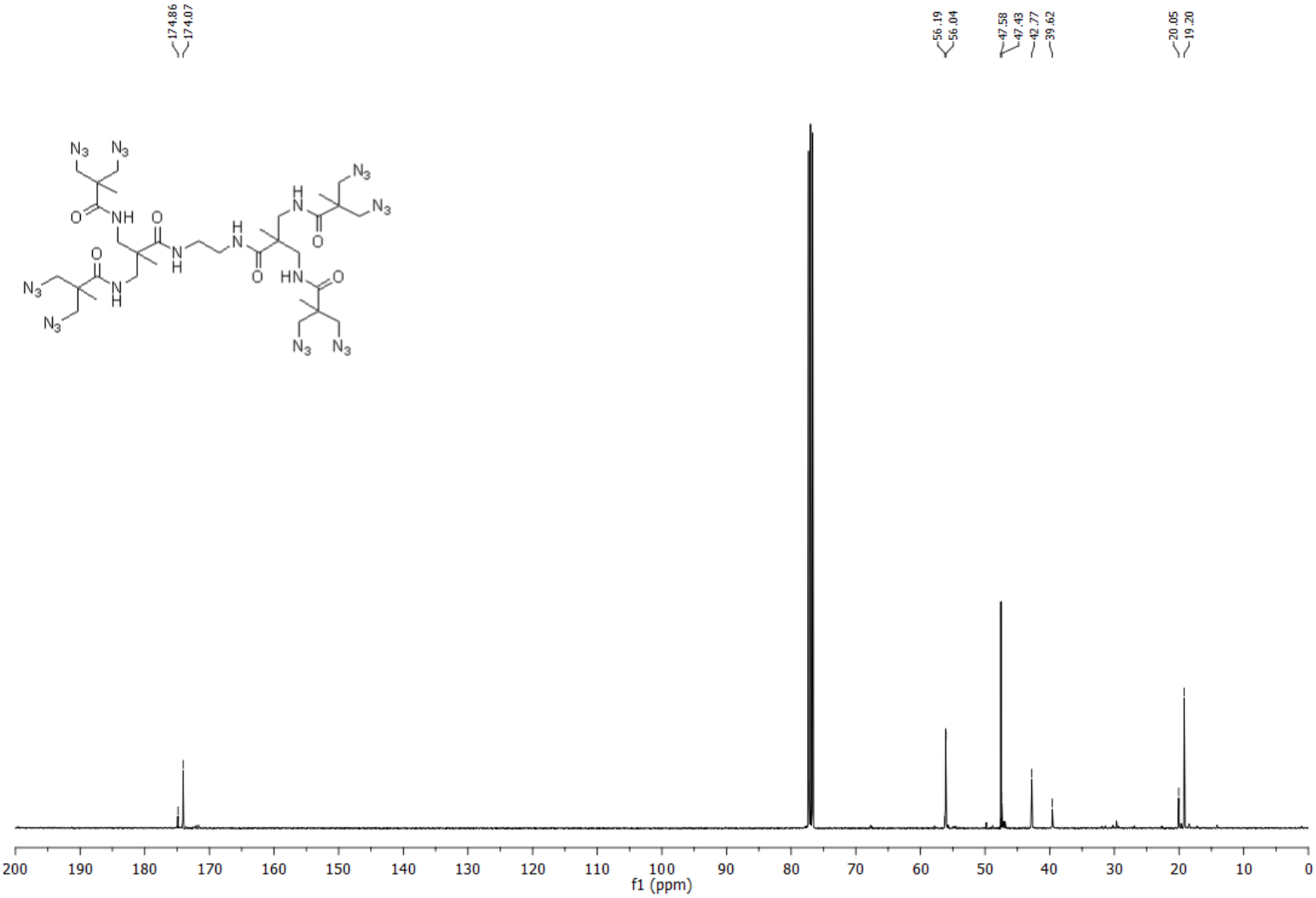

Fig. S12 ^{13}C-NMR spectrum (100 MHz, $CDCl_3$) of **G2-N_3**.

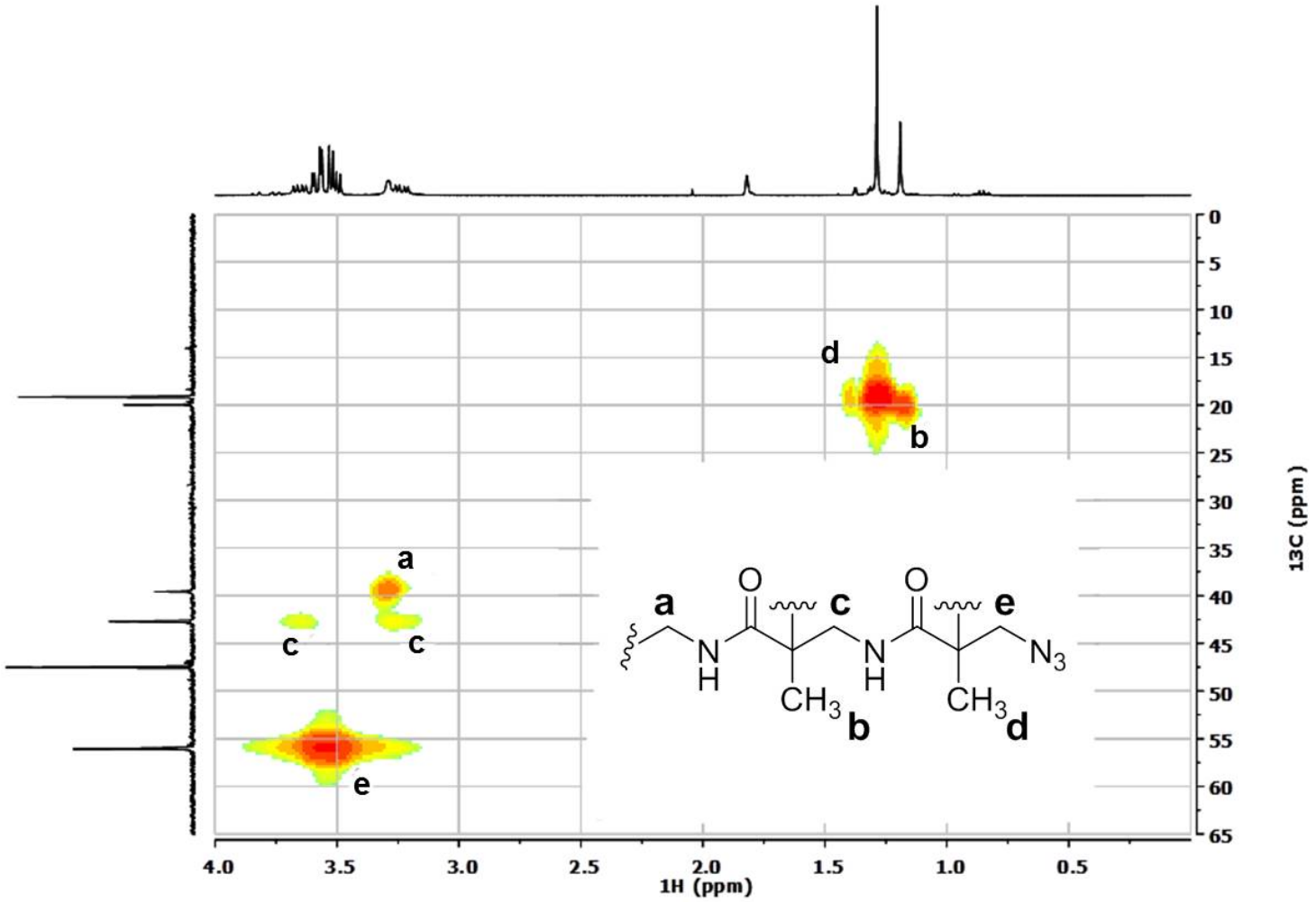

Fig. S13 HMQC-^{1}H-^{13}C spectrum ($CDCl_3$) of **G2-N_3**.

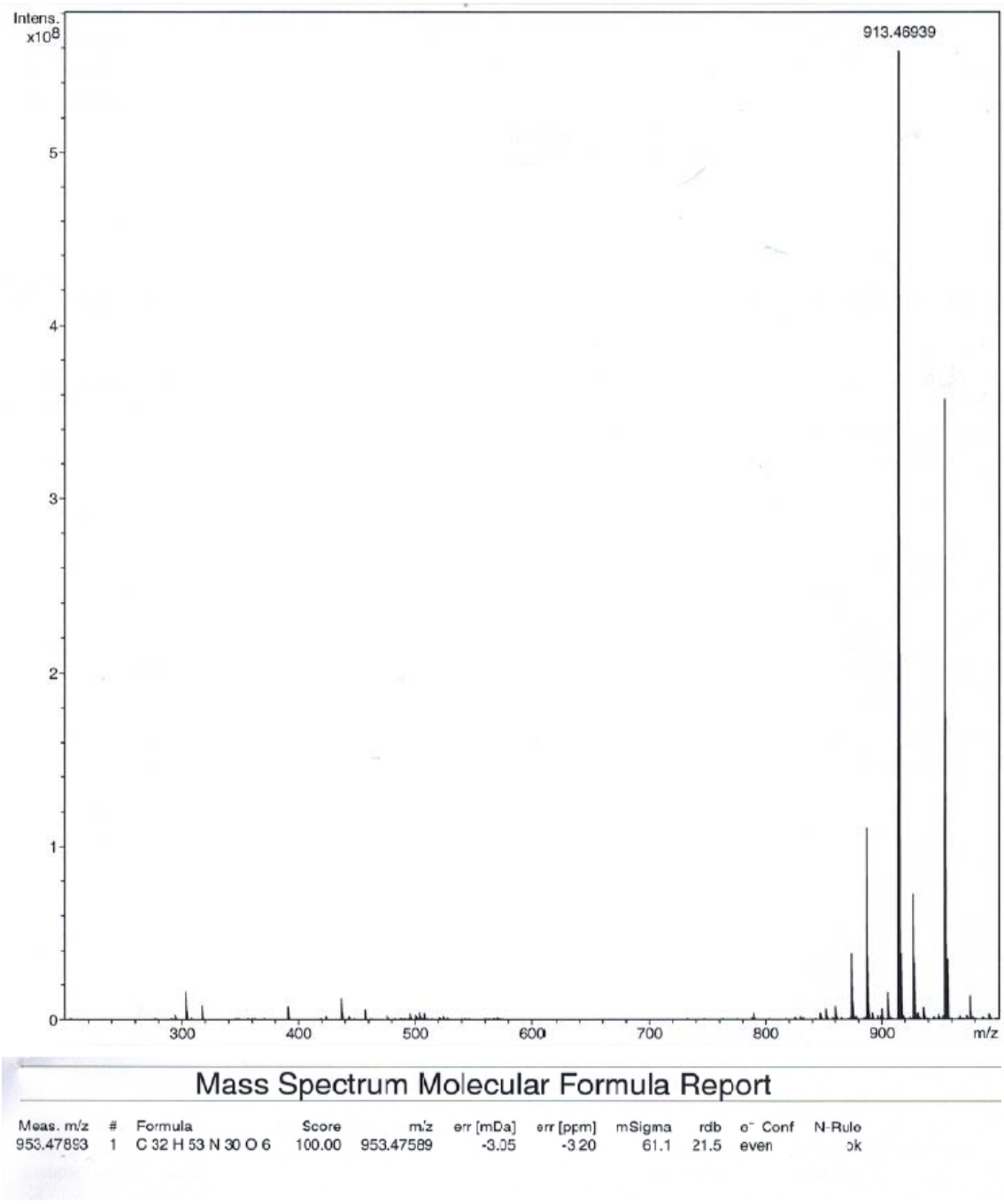

Mass Spectrum Molecular Formula Report

Meas. m/z	#	Formula	Score	m/z	err [mDa]	err [ppm]	mSigma	rdb	e⁻ Conf	N-Rule
953.47893	1	C 32 H 53 N 30 O 6	100.00	953.47589	-3.05	-3.20	61.1	21.5	even	ok

Fig. S14 ESI-TOF spectrum and Mass spectrum molecular formula report of **G2-N_3**.

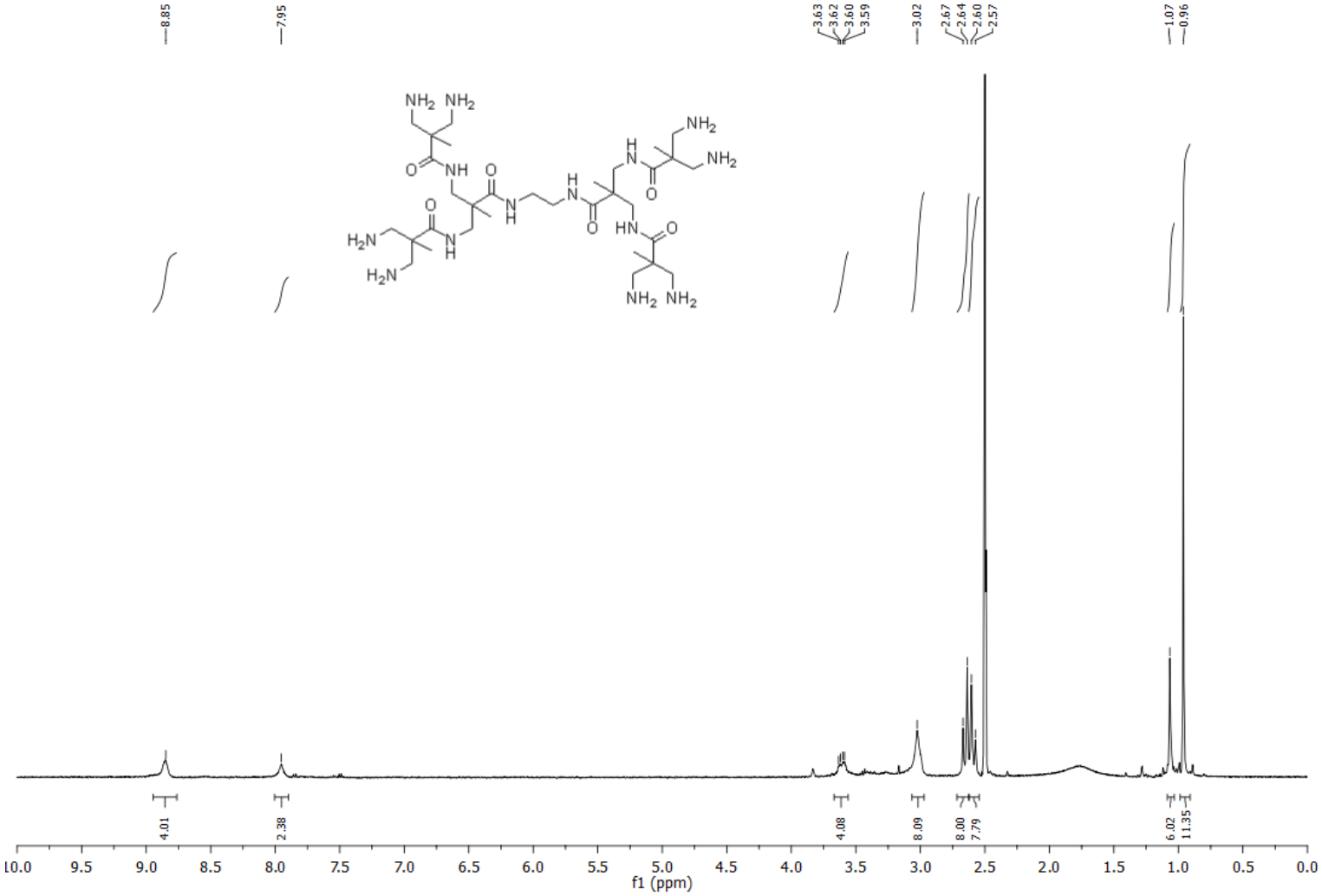

Fig. S15 ^{1}H-NMR spectrum (400 MHz, $(CD_3)_2SO$) of **G2-NH$_2$**.

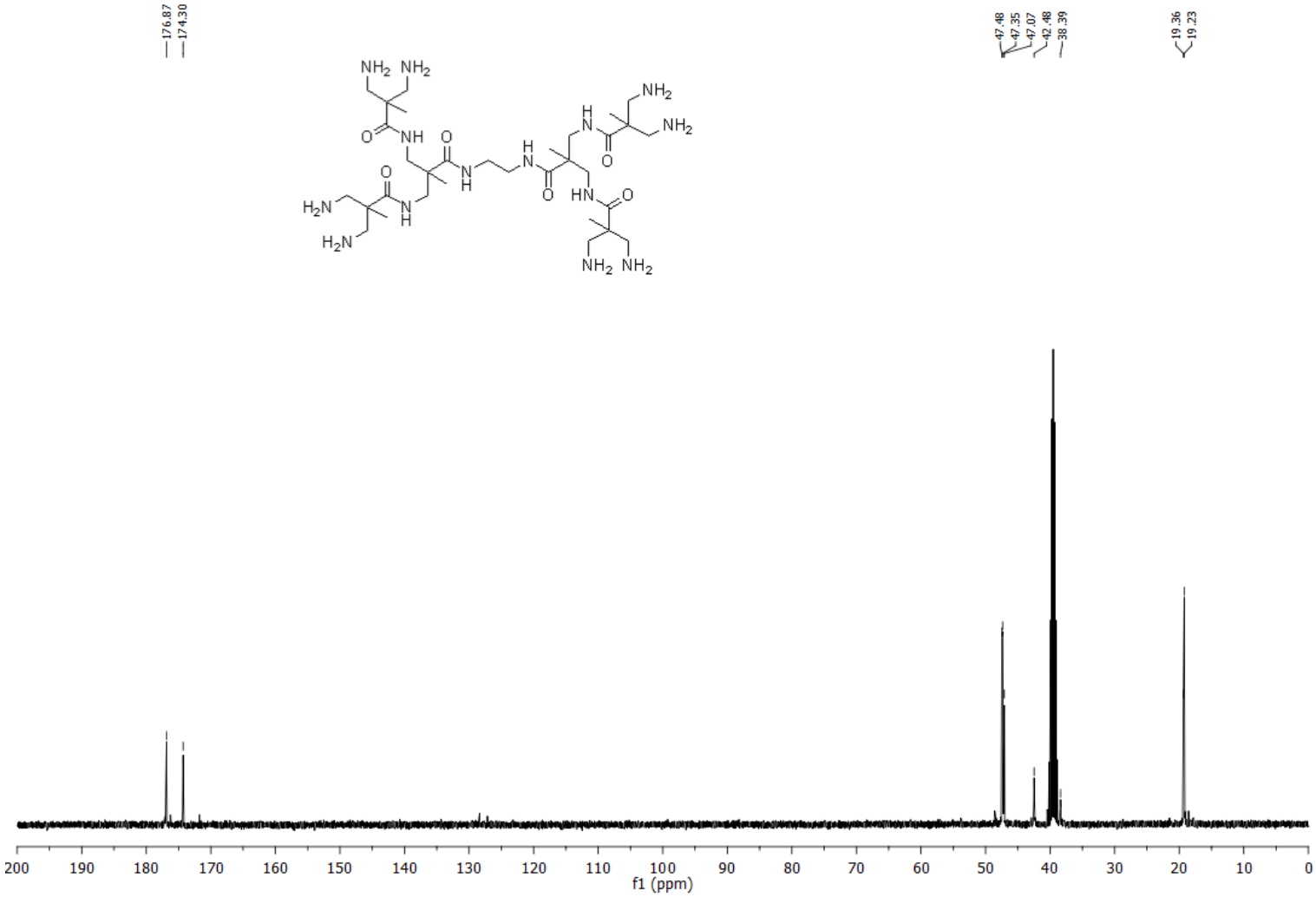

Fig. S16 ^{13}C-NMR spectrum (100 MHz, $(CD_3)_2SO$) of **G2-NH$_2$**.

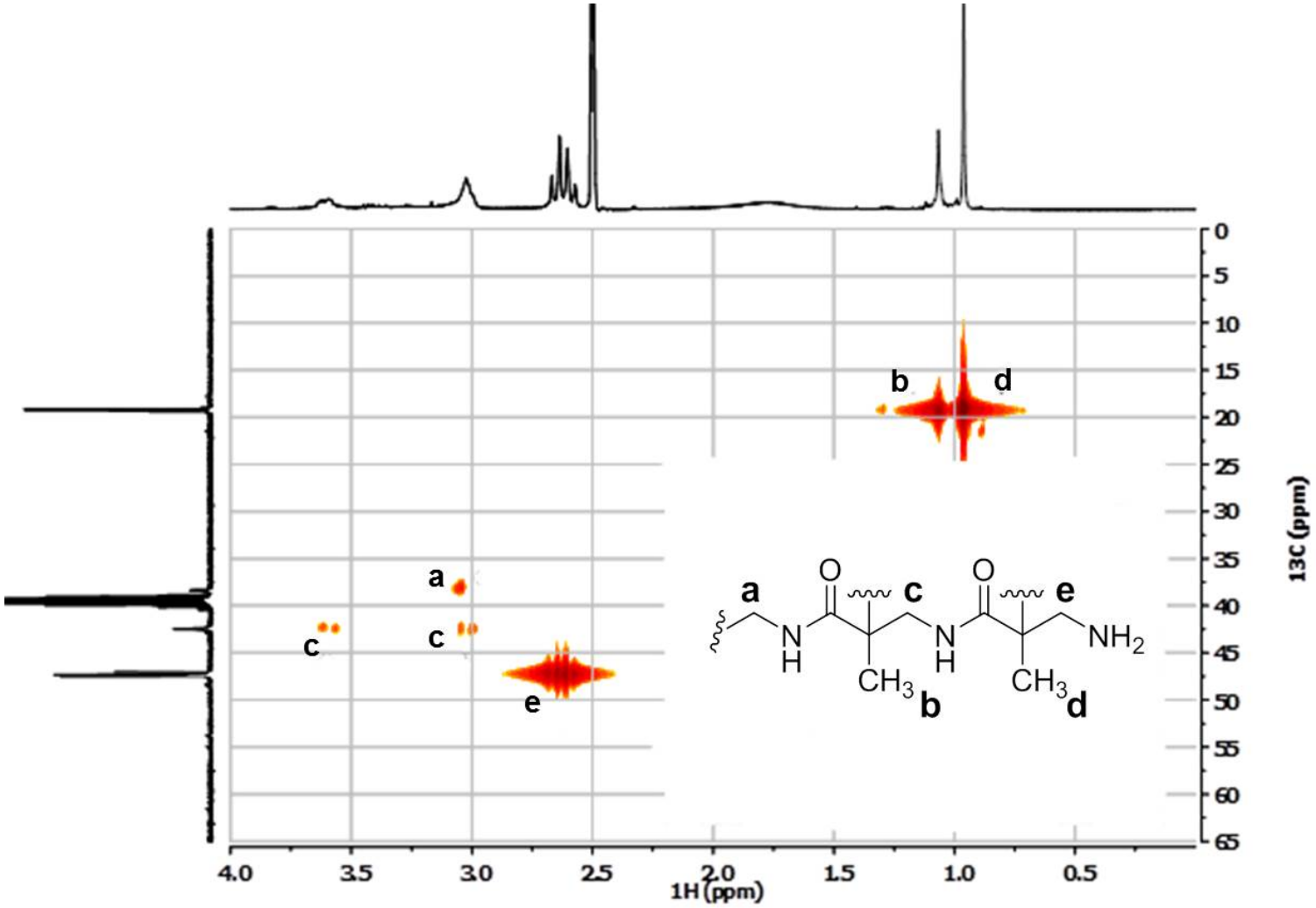

Fig. S17 HMQC-^{1}H-^{13}C spectrum $(CD_3)_2SO$) of **G2-NH$_2$**.

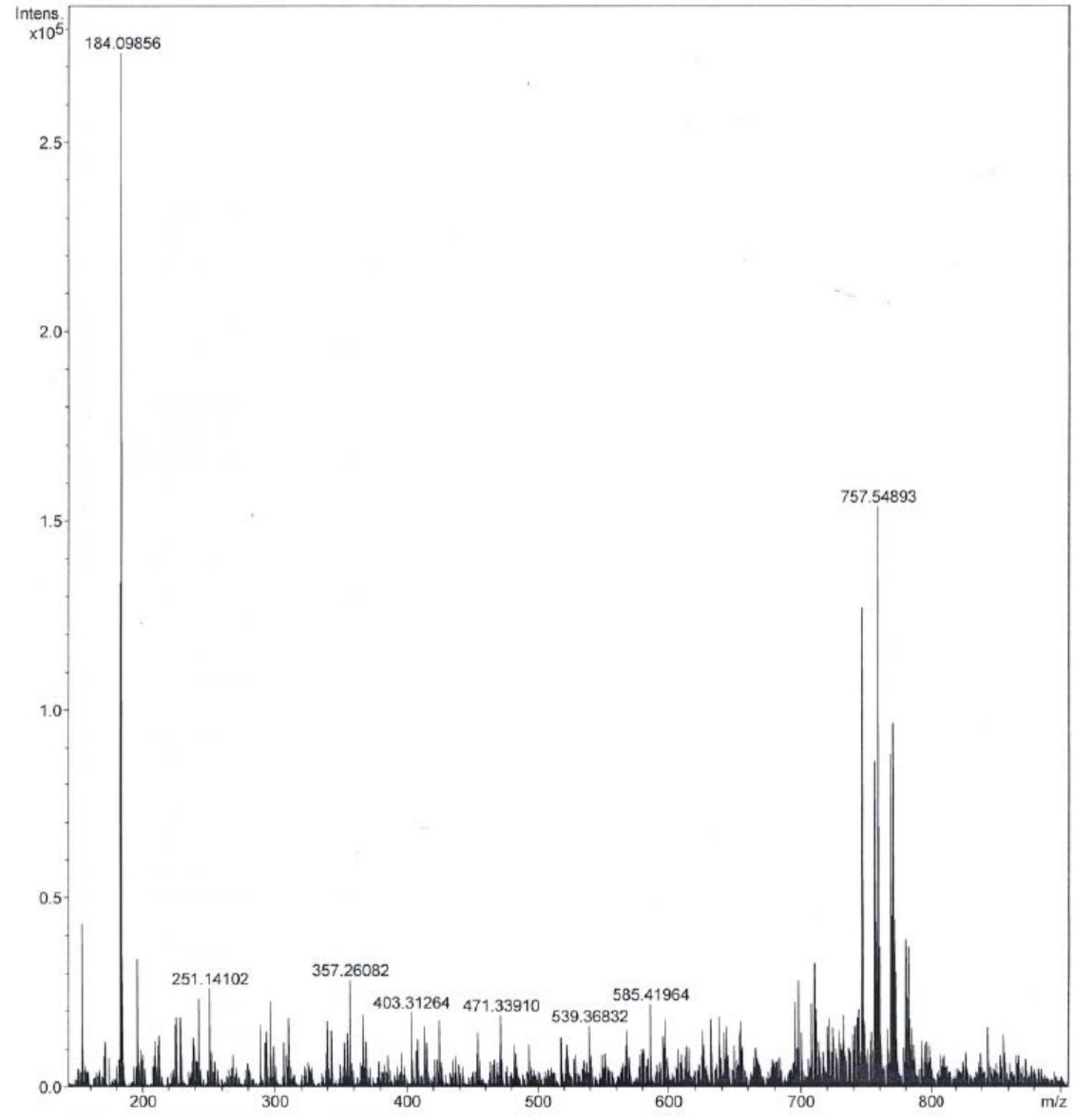

Mass Spectrum Molecular Formula Report

Meas. m/z	#	Formula	Score	m/z	err [mDa]	err [ppm]	mSigma	rdb	e⁻ Conf	N-Rule
745.55118	1	C 32 H 69 N 14 O 6	100.00	745.55190	0.7	1.0	29.7	5.5	even	ok
767.53258	1	C 32 H 68 N 14 Na O 6	100.00	767.53385	1.3	1.7	508.0	5.5	even	ok

Fig. S18 ESI-TOF spectrum and Mass spectrum molecular formula report of **G2-NH_2**.

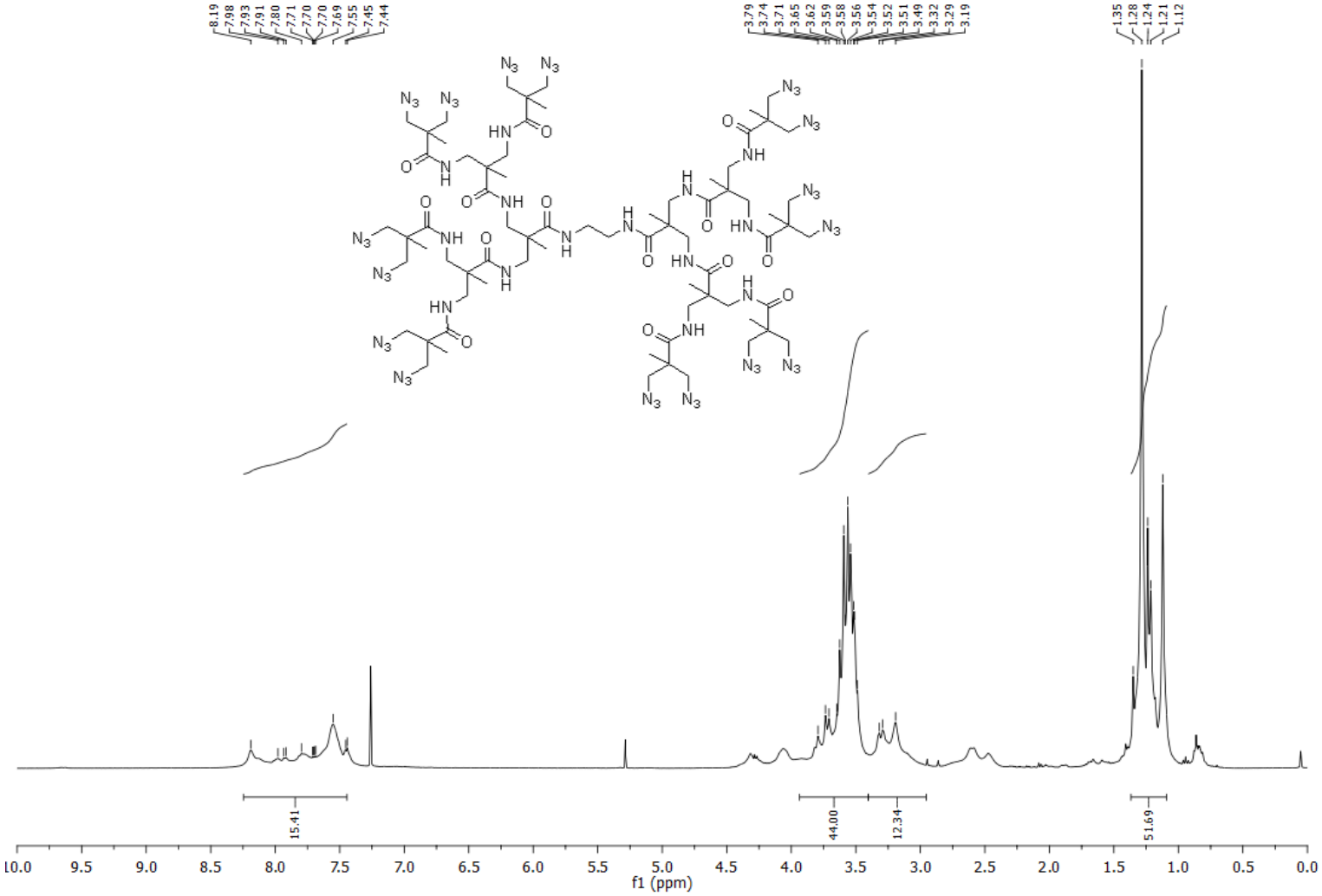

Fig. S19 ^{1}H-NMR spectrum (400 MHz, $CDCl_3$) of **G3-N_3**.

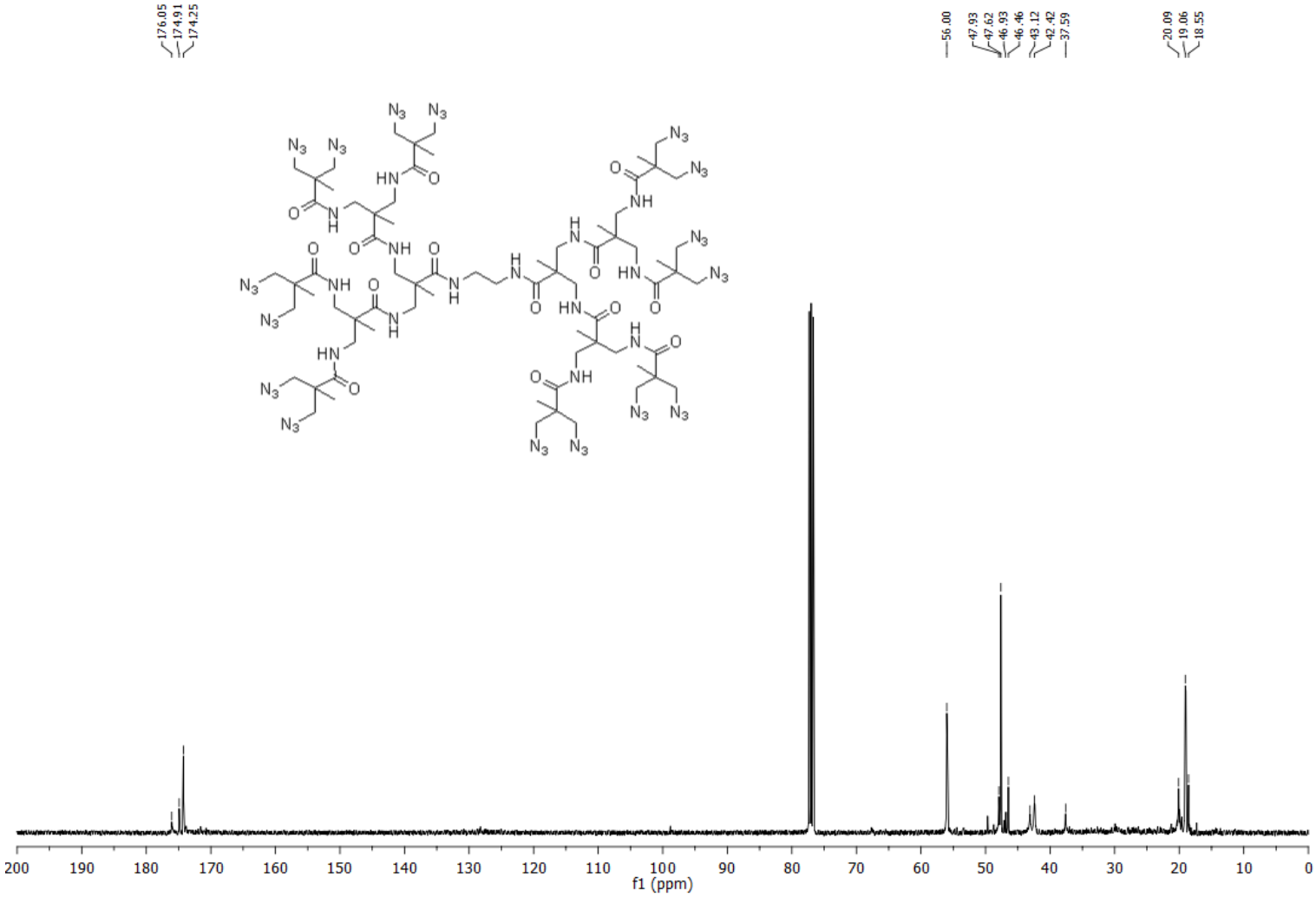

Fig. S20 ^{13}C-NMR spectrum (100 MHz, $CDCl_3$) of **G3-N_3**.

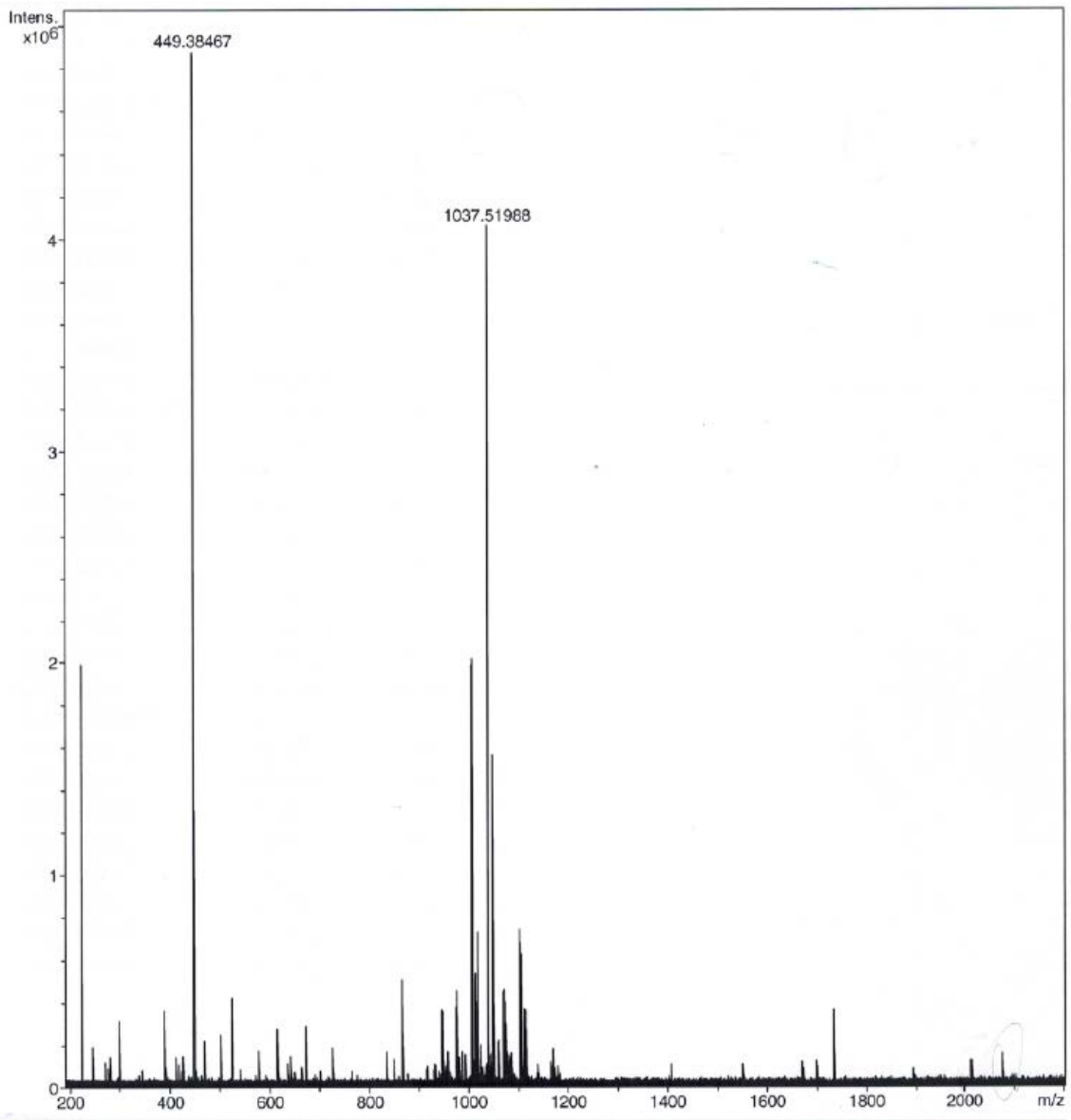

Mass Spectrum Molecular Formula Report

Meas. m/z	#	Formula	Score	m/z	err [mDa]	err [ppm]	mSigma	rdb	e⁻ Conf	N-Rule
1037.51988	1	C 70 H 116 N 65 O 13	100.00	1037.52015	0.27	0.26	37.1	45.5	odd	ok
	2	C 72 H 118 N 62 O 14	64.22	1037.52082	0.94	0.91	41.1	45.0	even	ok
	3	C 73 H 118 N 60 O 15	1.85	1037.51521	-4.67	-4.51	43.1	45.0	even	ok
	4	C 74 H 114 N 64 O 11	4.21	1037.51588	-4.01	-3.86	43.9	50.0	even	ok
	5	C 74 H 120 N 59 O 15	37.22	1037.52150	1.61	1.56	45.6	44.5	odd	ok
	6	C 75 H 116 N 63 O 11	21.96	1037.52216	2.28	2.20	46.4	49.5	odd	ok

Fig. S21 ESI-TOF spectrum and Mass spectrum molecular formula report of **G3-N_3**.

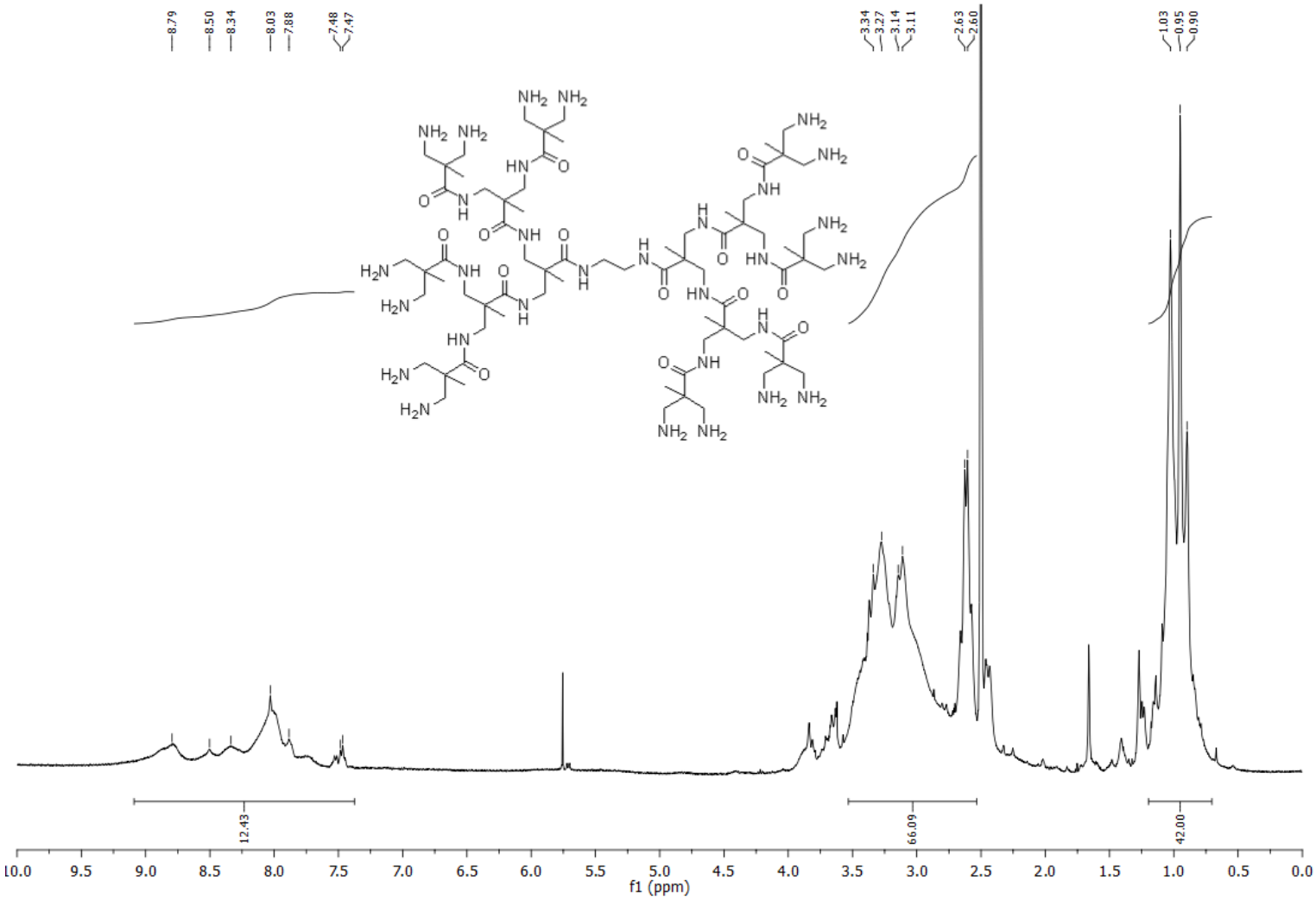

Fig. S22 ^{1}H-NMR spectrum (100 MHz, $(CD_3)_2SO$) of **G3-NH$_2$**.

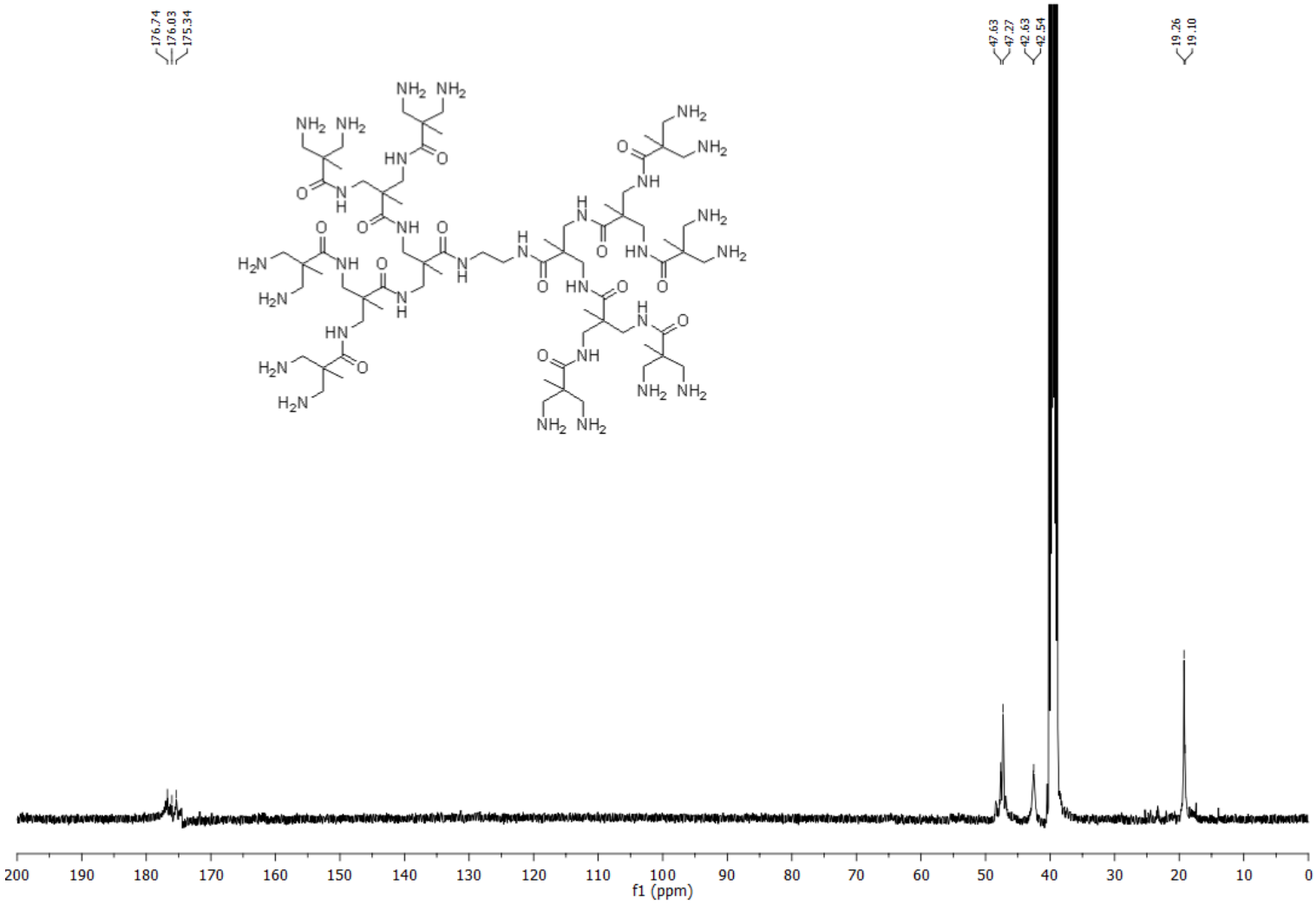

Fig. S23 ^{13}C-NMR spectrum (100 MHz, $(CD_3)_2SO$) of **G3-NH$_2$**.

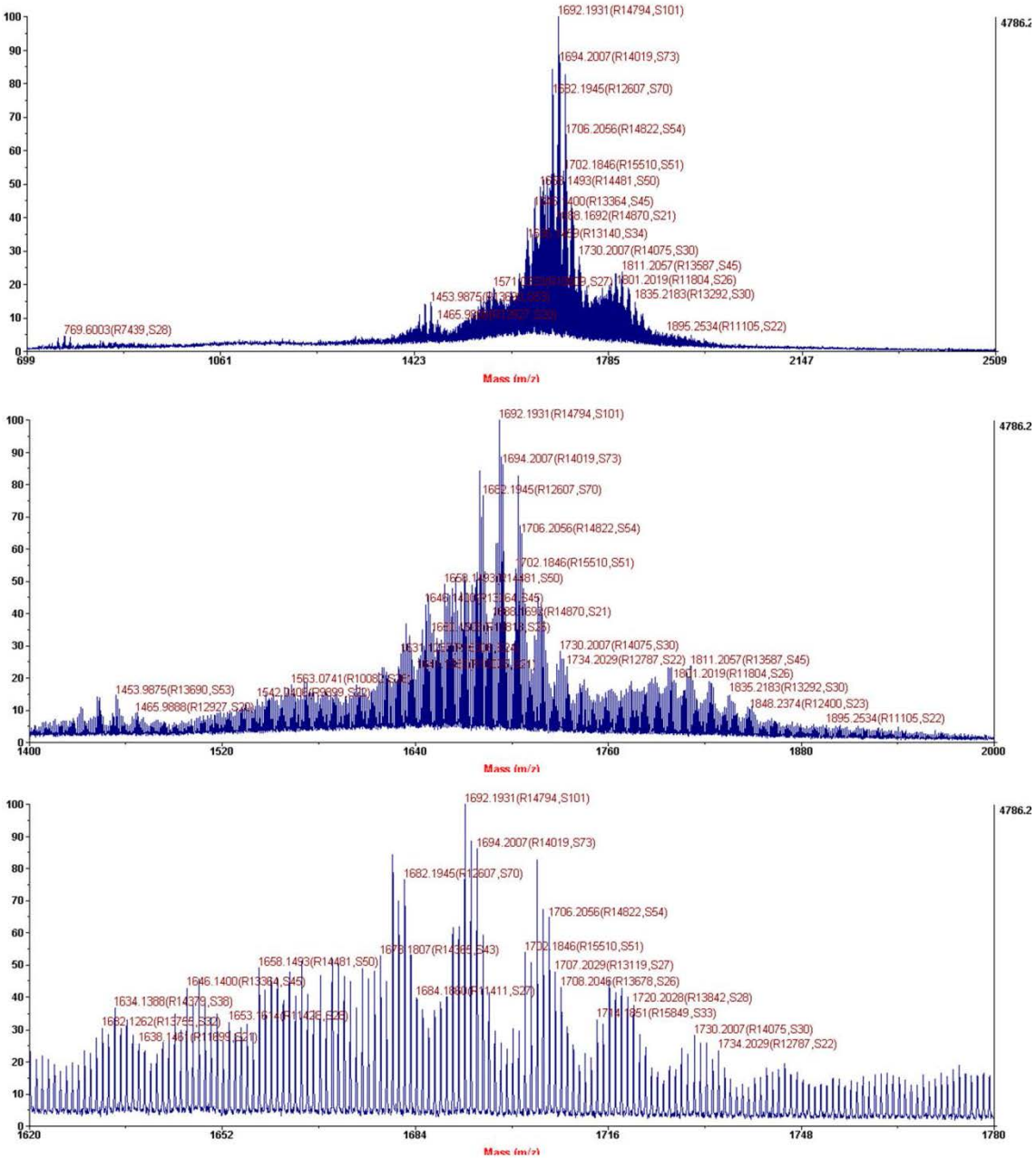

Fig. S24 MALDI-TOF spectrum and Mass spectrum molecular formula report of **G3-NH_2**.

4. TGA Experiments

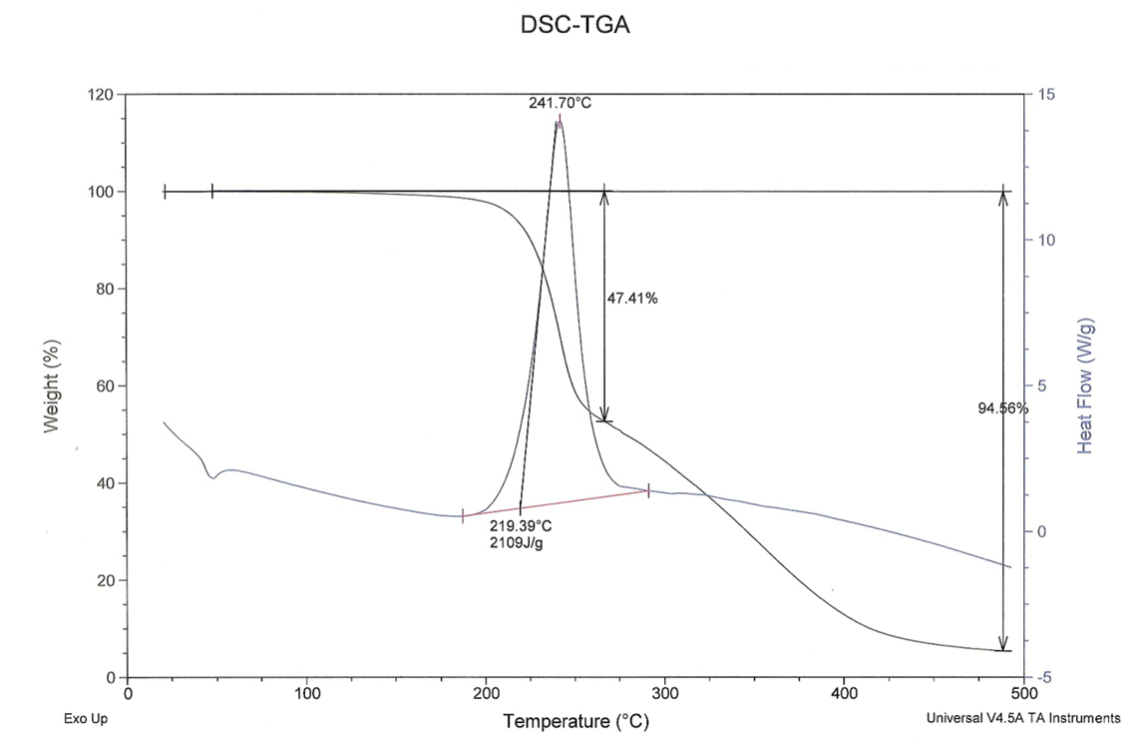

Fig. S25 TGA of **G1-N_3**.

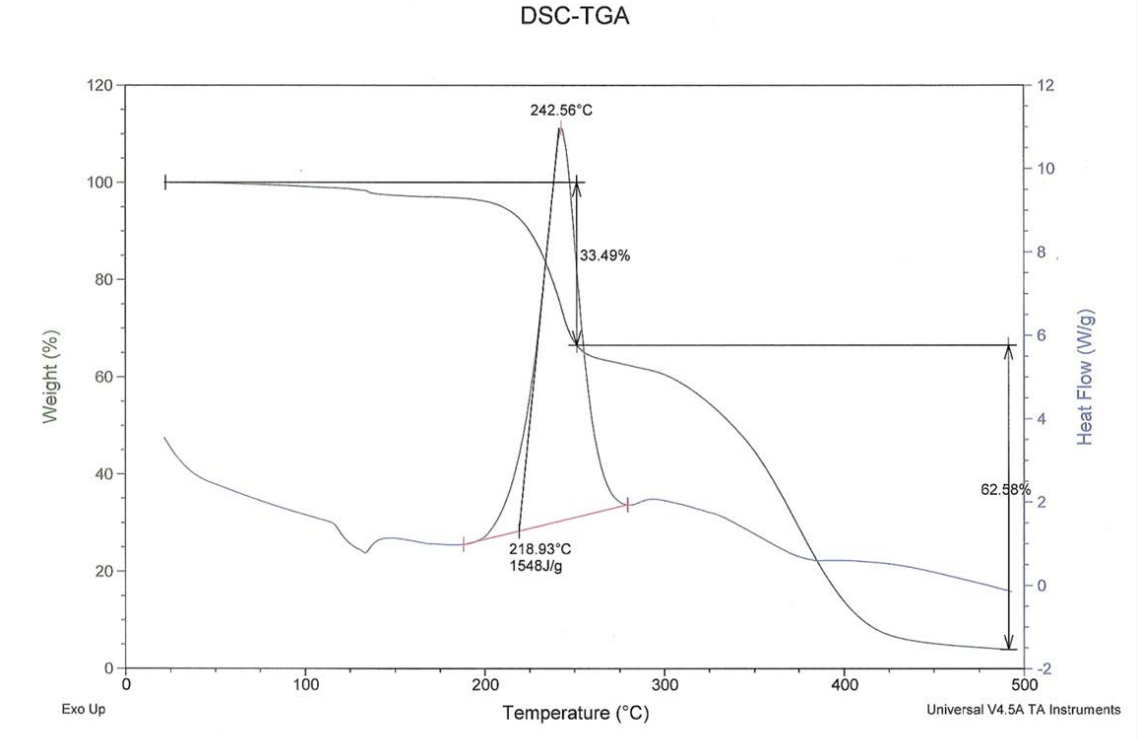

Fig. S26 TGA of **G2-N_3**.

5. Theoretical Calculations

Dendrimer Building. Gn-N_3 dendrimers are composed of three different residues: the ethylenediamine core (COR), repetitive 3,3'-diaminopivaloyl units (REP), and the terminal end 3,3'-diazidopivaloyl unit (TAZ). For the protonated Gn-NH_2 dendrimers the terminal residue was 3,3'-diamoniopivaloyl unit (TAM) (Figure S27).

For all of these residues a cap region was defined, and then removed before joining to another residue. For the azide group we used the parameter described previously.[3] For missing bonds, angle torsions, or van der Waals parameters not included in the parm99 force field, the values were transferred from the general AMBER force field (GAFF).[4] These moiety types were optimized and subjected to conformational analysis using TINKER-Software Tools for Molecular Design.[5] The minimum energy conformation was submitted to MP2/HF/6-31G(d) basis set calculation using G09,[6] (capped COR and REP residues were optimized *in vacuum*, while capped TAZ and TAM residues were optimized employing PCM-MP2/6-31G(d) with chloroform and water as solvents, respectively).[7] The restrained potential (RESP) method was used for charge fitting.[8] During charge calculation, total cap atom charge was constrained to zero, and the overall full residue charge was also set to zero except for the protonated residue (TAM), which was kept at +2. Decapped residues were created using the Antechamber module of Amber 12,[9] and used to build the desired dendrimer generation employing the Dendrimer Building Tool (DBT).[10]

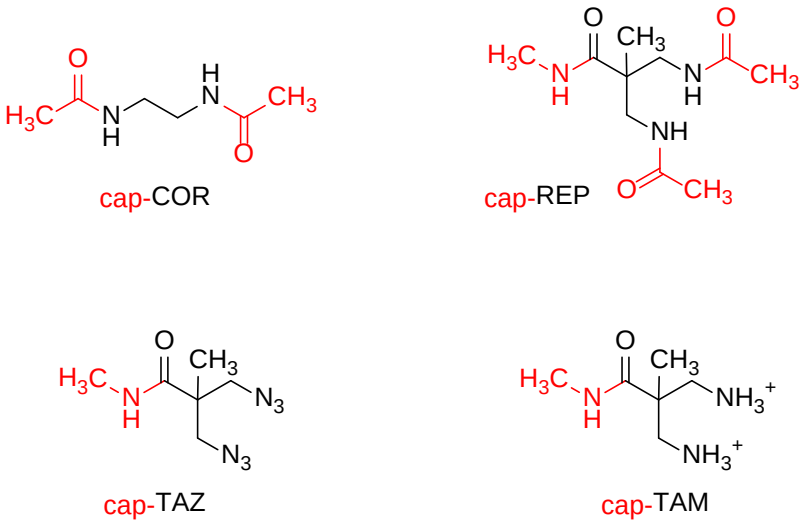

Fig. S27 Residue selection for Gn-N_3 and Gn-NH_2 dendrimers. Cap atoms are shown in red.

Simulation Details. For Gn-N_3 dendrimers, full atomistic simulations were performed in chloroform as explicit solvent. For Gn-NH_2 dendrimers, simulations were performed in water as explicit solvent at neutral pH. We used the AMBER 12 MD software package for all calculations.[9] To preserve overall charge neutrality and represent more realistic conditions for Gn-NH_2 dendrimers, an appropriate number of Cl^- counterions were added, and the molecules hydrated, using the TIP3P water model,[11] in truncated octahedral cells. In all cases the dimensions of these cells were chosen to provide a minimum 10 Å solvation shell around the dendrimer structure.

Table S1. Initial properties of dendrimers and simulation details. N_{den}, N_{Cl^-}, $N_{solvent}$ and N_{total} are, respectively, the number of dendrimer atoms, chloride ions, atoms in solvent molecules (chloroform for Gn-N_3 or water for Gn-NH_2) and the total number of atoms. V is the initial octahedral box volume.

Dendrimer	N_{den}	N_{Cl^-}	$N_{solvent}$	N_{total}	V(Å^3)
G1-N_3	48	--	*($CHCl_3$)* 905	953	35656
G2-N_3	120	--	*($CHCl_3$)* 1405	1525	52228
G3-N_3	264	--	*($CHCl_3$)* 2615	2879	93807
G1-NH_2	52	4	*(H_2O)* 5382	5438	64138
G2- NH_2	128	8	*(H_2O)* 7296	7432	88684
G3- NH_2	280	16	*(H_2O)* 12060	12356	146923

Solvated structures were minimized as described previously,[10] using six cycles of conjugated gradient minimization. During the initial cycle, dendrimers were kept in their starting conformation using a harmonic constraint with a force constant of 500 kcal/mol-Å^2. This was followed by another five periods of minimization while decreasing the harmonic restraint force constant from 20 kcal/mol-Å^2 to zero in steps of 5 kcal/mol-Å^2.

To allow a slow relaxation of the assembled dendrimer-solvent system, the minimized structure was heated slowly from 0 to 300 K with three steps of 40 ps of MD, the first of them under conditions of constant volume-constant temperature (NVT) and the rest under constant pressure-constant temperature (NPT) conditions. Initially, we applied a weak 20 kcal/mol-Å^2 harmonic constraint to the solute starting structure and slowly decreased it to zero in 5 kcal/mol-Å^2 steps. Finally, we carried out 2 ns of unconstrained MD simulation in NPT ensemble to equilibrate the system at 300 K. To solve the motion equation we used the Verlet leapfrog algorithm,[12] with an integration step of 2

fs. Bond lengths involving bonds to hydrogen atoms were constrained using the SHAKE algorithm,[13] using a geometrical tolerance of 5×10^{-4} Å.

Finally, starting from the configurations generated by the above procedure, production runs of 20 ns trajectories were performed under an NPT ensemble. Temperature regulation was achieved using the Berendsen weak coupling method (1 ps time constant for heat bath coupling and 0.5 ps for pressure relaxation time).[14] The particle-mesh Ewald (PME) algorithm was employed to treat long-range electrostatic interactions,[15] with a real space cut off of 9 Å. The same cutoff was used for van der Waals interactions. For the structural analyses (R_g, RDF, *etc*.) the last 1 ns equilibrated trajectory was used. Amber modules *ptraj* and *cpptraj* were used to accomplish these analyses. VMD software was used for the calculation of molecular surfaces.[16]

Autocorrelation function

Dendrimer relaxation was determined from the autocorrelation function of the squared radius-of-gyration, $C_{R_g^2}(t)$ which is evaluated from the expression: [17]

$$C_{R_g^2}(t) = \frac{\langle R_g^2(0) R_g^2(t) \rangle - \langle R_g^2 \rangle^2}{\langle R_g^4 \rangle - \langle R_g^2 \rangle^2}$$

The resulting graph is presented in Figure S28. In all cases $C_{R_g^2}(t)$ decays to 0 at time scales shorter than 1 ns, implying that the simulation times are sufficient to sample enough independent configurations in order to average static properties.

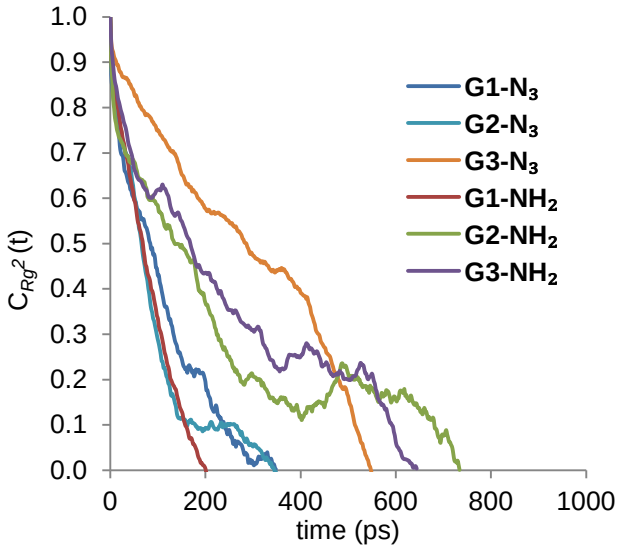

Fig. S28 Correlation functions of the squared radius of gyration for Gn-N_3 and Gn-NH_2 dendrimers.

Radius of gyration.

Dendrimer size can be quantified by considering the radius of gyration R_g of the molecular structure, computed as follows:

$$R_g = \left(\frac{\sum_i \|r_i\|^2 m_i}{\sum_i m_i} \right)^{1/2}$$

where m_i is the mass of atom i and r_i the position of atom $\boldsymbol{i}$ with respect to the molecule's center of mass.

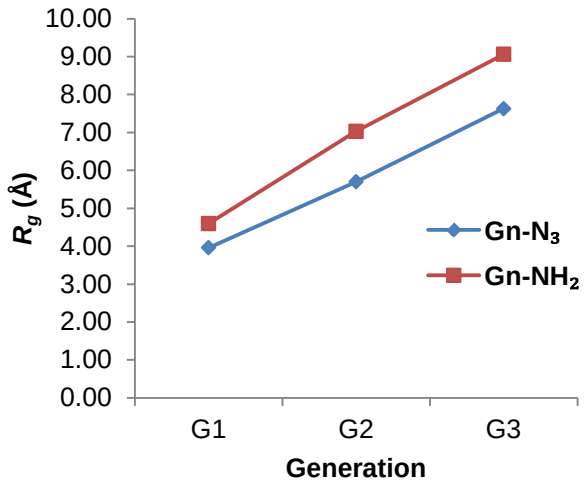

Fig. S29 Graph plotting Radius of Gyration against Gn-N_3 and Gn-NH_2 dendrimer generation.

Radius of the Solvent Accessible Surface Area (SASA)

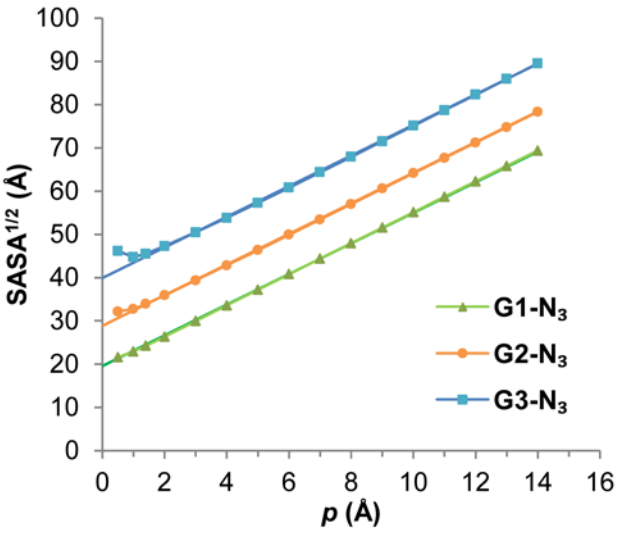

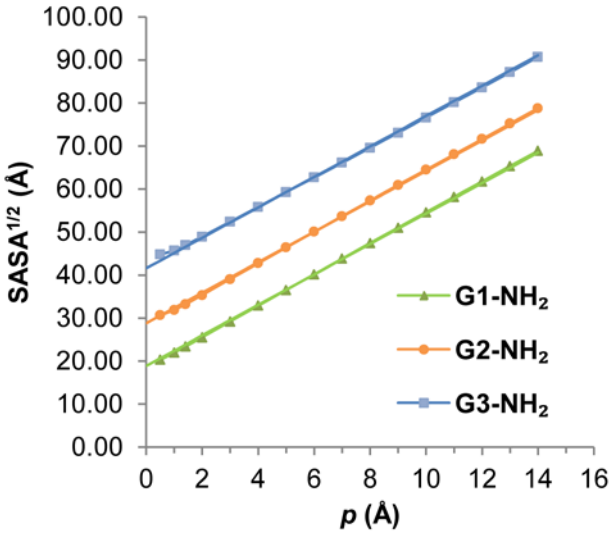

$SASA^{1/2} = a(R_{SASA} + p)$		
	a	R_{SASA} (Å)
G1-N_3	3.54	5.53
G2-N_3	3.54	8.16
G3-N_3	3.54	11.27

$SASA^{1/2} = a(R_{SASA} + p)$		
	a	R_{SASA} (Å)
G1-NH_2	3.54	5.34
G2-NH_2	3.54	8.14
G3-NH_2	3.54	11.75

Fig. S30 Square root of Solvent Accessible Surface Areas (SASA) as a function of probe radius *p* for Gn-N_3 dendrimers (a) and Gn-NH_2 dendrimers (b). A theoretical slope $(4\pi)^{1/2}$=3.54 was used.

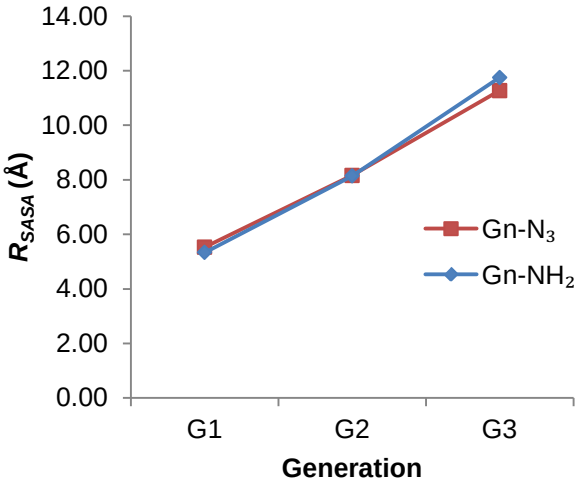

Fig. S31 Graph plotting Radius of the SASA against Gn-N_3 and Gn-NH_2 dendrimer generation.

Fractal dimension (d_f)

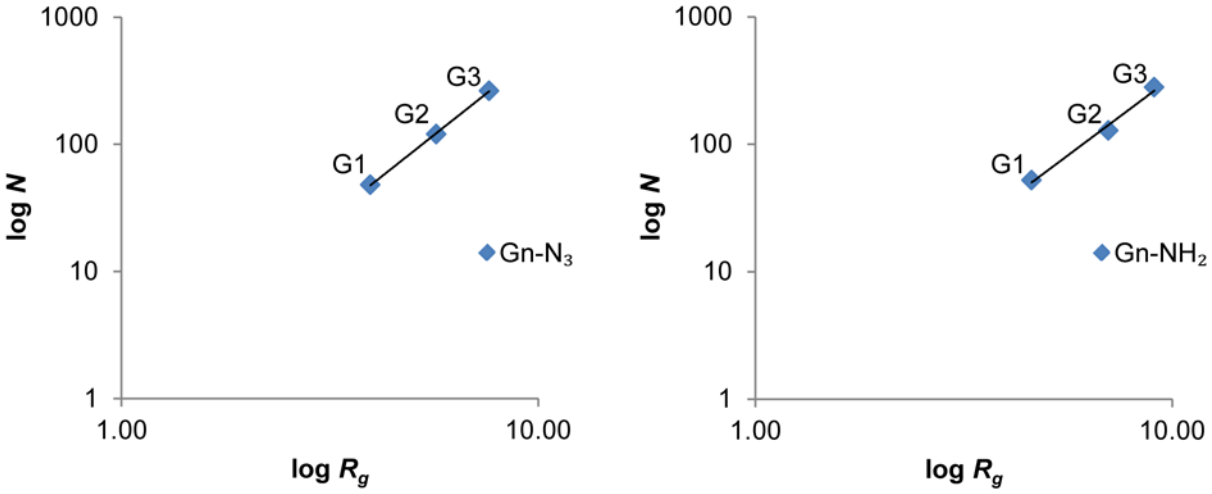

$N \sim R_g^{2.60}$ $N \sim R_g^{2.45}$

Fig. S32 Relationship between the number of atoms (N) of Gn-N_3 and Gn-NH_2 dendrimers and their R_g values.

Dendrimers shape

A structure-persistent characteristic of Gn-N_3 and Gn-NH_2 dendrimers can be obtained by considering average values of the three principal moments of inertia I_x, I_y, I_z (in descending order). Molecular asphericity was calculated as defined:[18]

$$\delta = 1 - 3\frac{\langle I_2 \rangle}{\langle I_1^2 \rangle}$$

where I_1 and I_2 are the first and second invariants of the radius of gyration tensor: $I_1 = I_x + I_y + I_z$, $I_2 = I_xI_y + I_yI_z + I_xI_z$. This quantity assumes values between 1 (for a linear array of atoms) and 0 (for shapes of high 3D similarity).

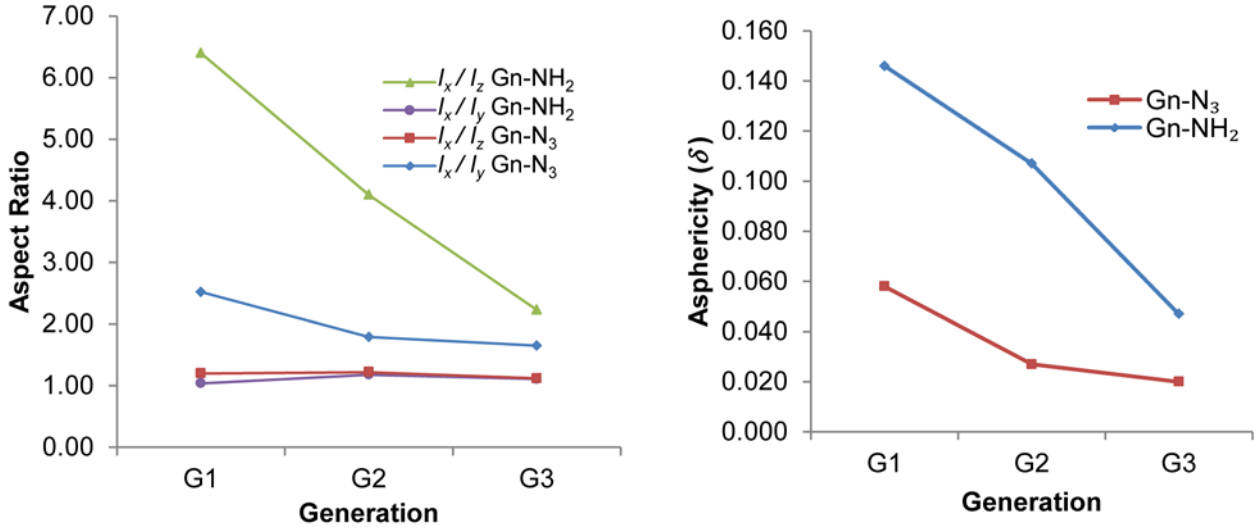

Fig. S33 Aspect ratios and asphericity values for Gn-N_3 and Gn-NH_2 dendrimers as a function of their generation.

Monomer radial distribution functions

Dendrimer conformation can be conveniently expressed through the average radial distribution function $\rho(r)$, which can be defined by counting the number *N(r)* of atoms whose centers of mass are located within the spherical shell of radius *r* and thickness Δr. Hence, integration over *r* yields the total number of atoms as: $N(r) = 4\pi \int_0^\infty r^2 \rho(r)\, dr$, where *r* is the distance from the dendrimer center of mass.

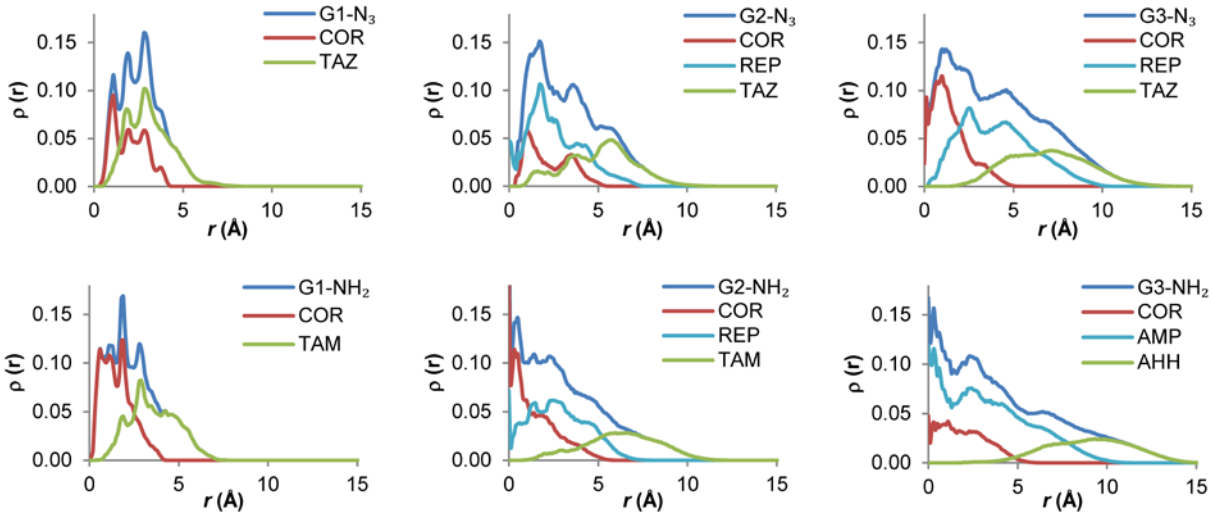

Fig. S34 Radial distribution function of Gn-N_3 and Gn-NH_2 dendrimers and its monomers using dendrimer center of mass as reference. The unit value for $\rho(r)$ is expressed in atoms/Å^3.

6. References

1 W. L. F. Armarego and Chai, C., *Purification of Laboratory Chemicals*, Butterworth-Heinemann, Amsterdam, 6th ed., 2009.

2 H. E. Gottlieb, V. Kotlyar and A. Nudelman, *J. Org. Chem.*, 1997, **62**, 7512–7515.

3 A. T. P. Carvalho, P. A. Fernandes and M. J. Ramos, *Int. J. Quantum Chem.*, 2007, **107**, 292–298.

4 J. Wang, R. M. Wolf, J. W. Caldwell, P. A. Kollman and D. A. Case, *J. Comput. Chem.*, 2004, **25**, 1157–1174.

5 J. W. Ponder, *TINKER - Software Tools for Molecular Design*, 2011. (http://dasher.wustl.edu/tinker/, accessed December 2014)

6 M. J. Frisch, G. W. Trucks, H. B. Schlegel, G. E. Scuseria, M. A. Robb, J. R. Cheeseman, G. Scalmani, V. Barone, B. Mennucci, G. A. Petersson, H. Nakatsuji, M. Caricato, X. Li, H. P. Hratchian, A. F. Izmaylov, J. Bloino, G. Zheng, J. L. Sonnenberg, M. Hada, M. Ehara, K. Toyota, R. Fukuda, J. Hasegawa, M. Ishida, T. Nakajima, Y. Honda, O. Kitao, H. Nakai, T. Vreven, J. A. Montgomery, Jr., J. E. Peralta, F. Ogliaro, M. Bearpark, J. J. Heyd, E. Brothers, K. N. Kudin, V. N. Staroverov, R. Kobayashi, J. Normand, K. Raghavachari, A. Rendell, J. C. Burant, S. S. Iyengar, J. Tomasi, M. Cossi, N. Rega, N. J. Millam, M. Klene, J. E. Knox, J. B. Cross, V. Bakken, C. Adamo, J. Jaramillo, R. Gomperts, R. E. Stratmann, O. Yazyev, A. J. Austin, R. Cammi, C. Pomelli, J. W. Ochterski, R. L. Martin, K. Morokuma, V. G. Zakrzewski, G. A. Voth, P. Salvador, J. J. Dannenberg, S. Dapprich, A. D. Daniels, O. Farkas, J. B. Foresman, J. V. Ortiz, J. Cioslowski and D. J. Fox, *Gaussian 09, Revision A.1*, Gaussian, Inc., Wallingford, CT, 2009.

7 J. Tomasi, B. Mennucci and R. Cammi, *Chem. Rev.*, 2005, **105**, 2999–3094.

8 C. I. Bayly, P. Cieplak, W. Cornell and P. A. Kollman, *J. Phys. Chem.*, 1993, **97**, 10269–10280.

9 D. A. Case, T. A. Darden, T. E. Cheatham, III, C. L. Simmerling, J. Wang, R. E. Duke, R. Luo, R. C. Walker, W. Zhang, K. M. Merz, B. P. Roberts, S. Hayik, A. E. Roitberg, G. Seabra, J. M. Swails, I. Kolossváry, K. F. Wong, F. Paesani, J. Vanicek, R. M. Wolf, J. Liu, X. Wu, S. R. Brozell, T. Steinbrecher, H. Gohlke, Q. Cai, X. Ye, J. Wang, M.-J. Hsieh, G. Cui, D. R. Roe, D. H. Mathews, M. G. Seetin, R. Salomon-Ferrer, C. Sagui, V. Babin, T. Luchko, S. Gusarov, A. Kovalenko and P. A. Kollman, *AMBER 12*, University of California, San Francisco, 2012.

10 V. Maingi, V. Jain, P. V. Bharatam and P. K. Maiti, *J. Comput. Chem.*, 2012, **33**, 1997–2011.

11 W. L. Jorgensen, J. Chandrasekhar, J. D. Madura, R. W. Impey and M. L. Klein, *J. Chem. Phys.*, 1983, **79**, 926–935.

12 L. Verlet, *Phys. Rev.*, 1967, **159**, 98–103.

13 J.-P. Ryckaert, G. Ciccotti and H. J. C. Berendsen, *J. Comput. Phys.*, 1977, **23**, 327–341.

14 H. J. C. Berendsen, J. P. M. Postma, W. F. van Gunsteren, A. DiNola and J. R. Haak, *J. Chem. Phys.*, 1984, **81**, 3684–3690.

15 T. Darden, D. York and L. Pedersen, *J. Chem. Phys.*, 1993, **98**, 10089–10092.

16 W. Humphrey, A. Dalke and K. Schulten, *J. Mol. Graph.*, 1996, **14**, 33–38.

17 G. K. Dalakoglou, K. Karatasos, S. V. Lyulin and A. V. Lyulin, *J. Chem. Phys.*, 2007, **127**, 214903.

18 J. Rudnick and G. Gaspari, *J. Phys. Math. Gen.*, 1986, **19**, L191.